© 2013. Published by The Company of Biologists Ltd | Development (2013) 140, 4830-4843 doi:10.1242/dev.100511

REVIEW

Mechanisms of scaling in pattern formation

David M. Umulis[1,*] and Hans G. Othmer[2,*]

ABSTRACT

Many organisms and their constituent tissues and organs vary substantially in size but differ little in morphology; they appear to be scaled versions of a common template or pattern. Such scaling involves adjusting the intrinsic scale of spatial patterns of gene expression that are set up during development to the size of the system. Identifying the mechanisms that regulate scaling of patterns at the tissue, organ and organism level during development is a longstanding challenge in biology, but recent molecular-level data and mathematical modeling have shed light on scaling mechanisms in several systems, including *Drosophila* and *Xenopus*. Here, we investigate the underlying principles needed for understanding the mechanisms that can produce scale invariance in spatial pattern formation and discuss examples of systems that scale during development.

KEY WORDS: Bone morphogenetic proteins, Mathematical modeling, Morphogen, Pattern formation, Scale invariance, Turing

Introduction

The variation or occurrence, often the regular occurrence, of some characteristic feature of a system in space or time is referred to as a pattern. Patterns occur at all levels of biological organization, from the cell to the population level (Fig. 1). Although the mechanisms that generate patterns at different levels vary in detail, they share some common features: there is a 'signal' that carries information and varies in space and/or time, there are mechanisms for communicating and detecting that signal, and there is a downstream mechanism that defines how the signal is interpreted. Of course, what the signal is and how it elicits a response differs from case to case, and here we restrict attention to spatial patterns in gene expression that arise during the early stages of embryonic development. In this context, the signals are morphogens, the communication involves transport through or around cells, and the interpretation and response may occur directly, if the signal is a transcription factor, or may involve a cascade of steps that lead to the control of gene expression. Importantly, these patterning processes can be influenced by the overall size of the tissue or organism.

When the patterning process is unaffected by the size of the system, and is determined solely by an intrinsic scale characteristic of the mechanism involved, more repetitions of the pattern element may be added as the system size increases, as occurs in certain fish patterns (Kondo and Asai, 1995; Painter et al., 1999) and in Turing mechanisms (see Glossary, Box 1). However, many organisms and their tissues and organs may vary substantially in size, but differ little in morphology and appear to be scaled versions of a common template or pattern. In other words, many systems can adjust the intrinsic scale of patterning in development to some measure of the size of the system. This phenomenon is referred to as global scaling, or simply scale invariance (see Glossary, Box 1). Scale invariance can be observed in many different contexts, ranging from the distribution of proteins in *Drosophila* embryos of different sizes, to the scaling of coat patterns on zebras (Fig. 1). Such scale invariance can be visualized with reference to a rubber sheet: a basic pattern dictated by the intrinsic scale is inscribed on the rubber sheet, and the sheet is then stretched isometrically to the final desired size, thus producing a scale-invariant pattern. This is an example of what is known as isometric scaling, which is a special case from the allometric scaling law (discussed below). In general, allometric scaling (see Glossary, Box 1) involves size-related correlations between different characteristics of a system (reviewed by Shingleton et al., 2007).

Our objective in this Review is to synthesize recent work on morphogen-mediated patterning mechanisms in systems that exhibit either exact or approximate scale invariance (Fig. 1), with a view towards identifying the principles of patterning mechanisms that can lead to a suitable degree of scale invariance in a growing tissue. To do this, we begin by providing an introduction to the general principles involved in mathematical models of pattern formation and scale invariance. We then focus on specific examples of systems that exhibit scale invariance and which illustrate the diversity of mechanisms that can produce it.

Modeling and mathematical analysis of pattern formation and scaling

In a widely studied class of patterning systems, a morphogen is produced at a specific location, transport is via diffusion, and the interpretation of the signal may involve a threshold mechanism. The French flag model (Box 2) is a paradigm of such reaction-diffusion mechanisms for morphogen-mediated spatial patterning and exemplifies a positional information mechanism (PI model; see Glossary, Box 1) (Wolpert, 1969). This model embodies the basic principles discussed in this Review, and we use it as a framework to describe an analytical approach, based on available experimental data, that leads to an understanding of several aspects of spatial pattern formation.

Size-related correlations between different characteristics or traits of a system, which can occur both within a species and between species, are usually described by a scaling law of the form $Y = Y_0 X^{\alpha} = Y_0 e^{\alpha \ln X}$, wherein X and Y are two traits of the system, and α is the exponent of the power law relationship between the traits (Shingleton et al., 2007). As will be elaborated later, the morphogen distribution in the French flag model can be cast into this general form. Of course, real systems are three-dimensional, and thus a single measure of size may not suffice; more complex relations may be needed to more accurately describe scaling. However, several ways in which morphogen patterning can be made scale invariant in one spatial dimension are illustrated in Fig. 2. For exponential morphogen distributions, the absolute distribution of morphogen

[1]Agricultural and Biological Engineering, Weldon School of Biomedical Engineering, Purdue University, West Lafayette, IN 47907, USA. [2]School of Mathematics and Digital Technology Center, University of Minnesota, Minneapolis, MN 55455, USA.

*Authors for correspondence (dumulis@purdue.edu; othmer@math.umn.edu)

Development (2013) doi:10.1242/dev.100511

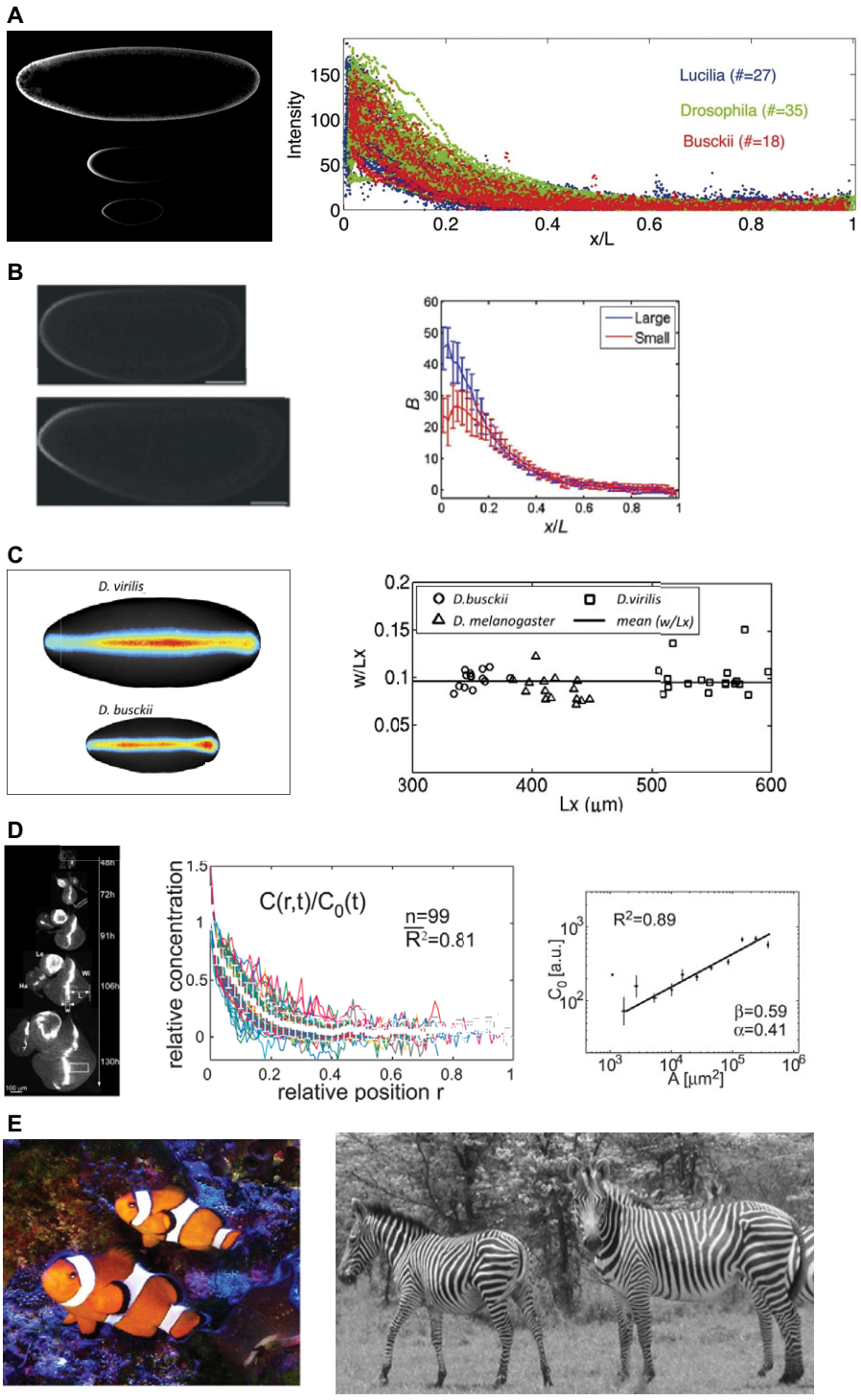

Fig. 1. Scale invariance of patterns in diverse contexts. (A) Interspecies scaling of the Bcd protein distribution in blastoderm embryos. Image (left) shows Bcd immunofluorescence stains for *Lucilia sericata* (top), *Drosophila melanogaster* (middle) and *Drosophila busckii* (bottom). The plot (right) shows the distribution of fluorescence in each species at relative spatial positions. Reproduced from Gregor et al. (Gregor et al., 2005). (B) Intraspecies scaling of the Bcd gradient in *Drosophila melanogaster* populations that have undergone rounds of artificial selection based on egg size. The image (left) shows a large embryo (bottom) and a small embryo (top). Image brightness was enhanced for clarity. The plot (right) shows the relative Bcd staining intensity for large and small embryos as a function of relative spatial position. Reproduced with permission (Cheung et al., 2011). (C) Scaling of dorsal surface patterning by bone morphogenetic proteins is an example of a complex, highly non-linear spatial patterning system. The image (left) shows the distribution of pMad in a large *Drosophila virilis* embryo (top) and a small *Drosophila busckii* embryo (bottom). The plot (right) shows the ratio of average pattern width to embryo length versus the embryo length. A threshold of signaling intensity of 0.2 was used for comparison of widths. Adapted with permission (Umulis et al., 2010). (D) Scaling of the Dpp gradient during growth of the wing imaginal disc is an example of dynamic scaling. The image (left) shows Dpp-GFP expression at various time points during development. Normalized Dpp-GFP profiles from multiple time-points (center) are shown at relative spatial positions. During growth, the amplitude of the morphogen gradient grows (right) in proportion to the length of the disc squared. Adapted with permission (Wartlick et al., 2011). (E) Pigmentation patterns on the skin of the clownfish *Amphiprion percula* (left; photo by D. M. Umulis) and coat patterns on zebras (right). Zebra image reprinted with permission (Cordingley et al., 2009).

range would not change if there is no size compensation (Fig. 2A,B), and the profiles extend into the tissue the same distance on an absolute scale and a shorter distance on a relative scale. If more morphogen is supplied to the system, the 'shape' or decay length of the morphogen is constant, yet some scaling is provided that depends primarily on the distance from the source (Fig. 2C,D). Lastly, processes that target both the biophysical properties that affect morphogen range and the production of the morphogen from the source can achieve 'perfect' scaling (Fig. 2E,F). As we discuss below, a simple breakdown of the components involved in generating a pattern, together with mathematical analysis of how these components interact, can help to identify the mechanisms that can achieve such 'perfect' scaling during development.

Patterning system modules

Many developmental patterning systems, including the French flag model (Box 2), involve four interacting modules: (1) a source module that generates the morphogen signal; (2) a transport module for redistributing the morphogen; (3) a reaction module that interacts with transport to shape the morphogen distribution; and (4) a module for detection and transduction of the signal, interpretation of the transduced signal, and initiation of a response (Fig. 3). Extensive

Development (2013) doi:10.1242/dev.100511

Box 1. Glossary

Allometric scaling. Changes in size lead to changes in proportion between two measured quantities. Isometric scaling of certain pattern characteristics (the rubber sheet analogy in the text) is a special case.

Chemical wavelength. An intrinsic scale of a pattern commonly used to refer to the distance between repeating stripes as occurs in some Turing mechanisms.

Constitutive equation. A mathematical relationship (often empirically derived) that describes the interaction between two physical quantities. Fick's law of diffusion (see below) is a constitutive equation. Other constitutive equations could relate growth of a tissue to the concentration of a morphogen.

Continuity equation. A mathematical relationship that equates the local rate of change of the density or concentration of a species to all changes, such as transport and reaction, that alter the amounts of that species.

Diptera. Insects of the order *Diptera*, which means 'two wings'; commonly referred to as the 'true flies'.

Extensive property. A property or value that depends on the size or amount of the system (e.g. the total number of molecules).

Fick's law of diffusion. A mathematical relationship for the net flux of material from high to low concentration at a rate proportional to the spatial gradient of the concentration.

Flux. For mass transport, it is the rate of material flow through a surface that defines a control volume. For reactions, it is the rate at which material is converted.

Intensive property. A property or variable that is independent of the size or amount of the system (e.g. the concentration of a molecule).

Positional information mechanism. A spatial patterning mechanism that posits that a cell 'knows' its position in a tissue by sensing the local value of a morphogen (Wolpert, 1969).

Scale invariance. The preservation of proportion for a tissue, structure or feature with respect to changes in overall system size or length.

Turing mechanism. A spatial patterning mechanism based on a reaction-diffusion system that has an unstable uniform state and a stable non-uniform state. These mechanisms frequently lead to stable patterns of stripes and spots reminiscent of pigmentation patterns in animal coats.

theoretical work in a variety of systems has focused on the fourth module, which we call the detection-transduction-response (DTR) module (Fig. 3) (Milo et al., 2002; Alon, 2007; Hecht et al., 2009). Evolution has shaped selected properties of the DTR modules to interpret, and in some instances regulate, the extracellular distribution of morphogens in order to achieve the ability to scale appropriately to the size of the system. Of course, the structure of DTRs is dependent on the spatiotemporal characteristics of the source module: is the morphogen generated spontaneously within the tissue or are the sources located at the boundary or at specialized regions within the interior of the tissue? The structure of the DTR is also influenced by the transport mechanism used to communicate information throughout the system. Thus, although the details of the components in these modules vary enormously between systems, scale invariance of the patterns generated by these modules is a fundamental property that can be understood by applying general principles that underlie all systems. Furthermore, thinking about complex patterning systems in this compartmentalized way can facilitate our understanding of the effect of distinct processes and their interactions on the overall outcome (Kang et al., 2012). Although we simplify the discussion by considering only one cycle of the integrated signal/transport/response system, we should emphasize that development is hierarchical in both space and time, that frequently gene expression is transient, and that one patterning system typically initiates a successor.

The governing equations of morphogen patterning

The properties of the four modules of a patterning system can be translated into a mathematical model that can then be used to predict the spatiotemporal evolution of the morphogen(s) and the downstream response. The source module is dependent on the specific system. There can also be numerous modes of transport in patterning systems (as discussed in detail below), and each type of transport involved has a direct effect on the scaling properties of the spatial patterns that emerge for a particular type. In the DTR module, signal detection via receptor binding, internalization, and the resulting downstream steps typically involves first- or second-order biochemical reactions, examples of which are given later. A general mathematical analysis of scale invariance is developed in supplementary material Boxes S1-S5 in Appendix S1, but the essential principles that underlie scaling can be understood by considering each of the components in a patterning system in turn.

The concentrations, reaction rates and diffusion constants of morphogens and other components of the DTR are intensive properties (see Glossary, Box 1), and thus, by definition, are independent of the size of the system. The material flux that stems from transport processes is an extensive property (see Glossary, Box 1) and is therefore dependent on the spatial variation of the component being transported, which introduces a length scale. The interaction between scale-independent processes, such as binding and chemical reaction, and scale-dependent transport processes defines an intrinsic length scale, called the chemical wavelength (see Glossary, Box 1), that reflects the functional range of a morphogen (Turing, 1952; Othmer and Scriven, 1969), or the decay length in simple versions of PI models. In a cell-based description, this wavelength is measured in numbers of cells (Othmer and Scriven, 1971), but the length scales of interest here involve many cell diameters, and thus a 'homogenized' description of the cells introduces a spatial length scale (Othmer, 1983; Bollenbach et al., 2008). Because intrinsic scales are independent of the system size, additional mechanisms that reflect the size are needed in the patterning mechanism, and the central problem that can be addressed with mathematical models is the identification of mechanisms that can achieve this.

In order to identify such mechanisms, we must first formulate the balance equations that determine how the transport processes and the steps in a DTR interact to produce the morphogen concentration throughout space as a function of time. In so doing, we can begin to understand how the different processes in the patterning system interact, and determine how the spatial extent of the system affects the balance of processes that establish the morphogen distribution.

The first process that dictates the type and range of morphogen pattern is spatial transport, which can occur in many ways, including diffusion, advection or flow, and active transport by biochemical processes. Because transport can occur in many different geometries that may include physical barriers, geometry may reduce the overall transport rates (Fig. 4) (reviewed by Müller et al., 2013). The basic accounting principles that determine how the morphogen transport module and the kinetics module interact are embedded in what is called the equation of change for mass or simply the continuity equation (see Glossary, Box 1). To derive it, imagine a small volume in the system and focus on the amount of a particular species in that volume. The total amount of this species is the integral over the volume of the density or concentration of the species, and this can change in only two ways: either in response to chemical conversion within the system, which may involve chemical reaction but also may occur as a result of binding to a receptor if the species is a ligand, or in response to influx or outflow across the boundary of the volume, which involves one or more transport steps. By equating the rate of change of the total amount of the species to the changes

Development (2013) doi:10.1242/dev.100511

Box 2. The French flag paradigm for morphogen patterning

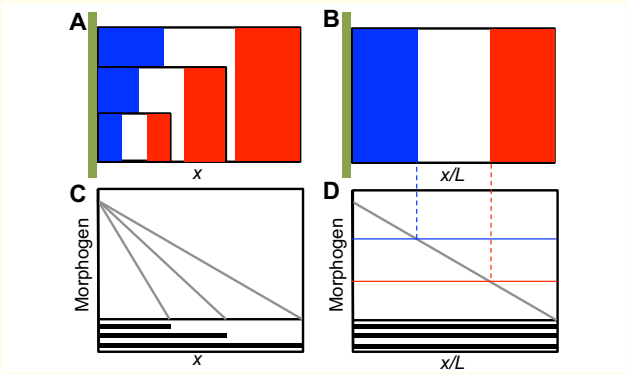

The French flag model of pattern formation emerged as the unification of the concepts of induction field theory in which a cell instructs its neighbors to adopt a specific type and positional information whereby a cell is assigned or 'knows' its positions relative to other cells. Gradients of material emerged as a possible explanation of induction that could provide information to cells in a field. The unified theory posits that cells respond to the inductive material and adopt a particular fate consistent with the level of morphogen and their current cellular state that itself is a function of that cell's history. The French flag model has evolved to support a physical interpretation whereby cells at the source (A,B, green vertical bar) secrete the inductive molecule (morphogen), which is transported over the field of cells by diffusion, convection, or cell-mediated active transport processes. Cells primed to receive instruction then incorporate the material information into the regulation of gene expression, presumably by a thresholding mechanism (B,D). A fundamental question has since emerged pertaining to the reliability of morphogen-mediated patterning to pattern tissues proportionately (A) such that the positions of gene expression are spaced equally when scaled by the overall system size (B). A number of mechanisms have been proposed to accomplish the preservation of proportion or 'scale invariance' and an update to the French flag paradigm is in order. In the modified paradigm, the 'positional information' concept now includes dynamic evolution of cellular context and receptivity to the morphogen whereby cells are constantly responding to and modifying the morphogen signal and their own interpretation of the morphogen signal via feedback mechanisms.

due to reaction or transport we arrive at a statement of conservation of mass in the volume. In an additional step that assumes that the spatial distribution of the species varies smoothly, one can reduce the integral form of the continuity equation to the following local form in Cartesian coordinates:

$$\frac{\partial c_i}{\partial t} = -\left(\frac{\partial j_{i,x}}{\partial x} + \frac{\partial j_{i,y}}{\partial y} + \frac{\partial j_{i,z}}{\partial z}\right) + R_i \,, \qquad (1)$$

wherein $j_{i,k}$, $k = x, y, z$ are the fluxes of species i due to all transport steps in the respective coordinate directions, and R_i contains all the reaction steps that affect the ith species. This equation is simply a formal statement of the conservation of mass in a system of fixed size, and is valid for all morphogen-patterning mechanisms in such systems. The concentration c_i can be measured in moles/unit-volume, the fluxes $j_{i,k}$ are then measured in moles/unit-area/unit-time, and R_i is the net rate of production of the component in moles/unit-volume/unit-time, which involves kinetic rate constants and the concentration of other species (supplementary material Box S1 in Appendix S1). When the system is growing, perhaps owing to cell division, additional equations must be incorporated in the model to reflect growth (Othmer et al., 2009).

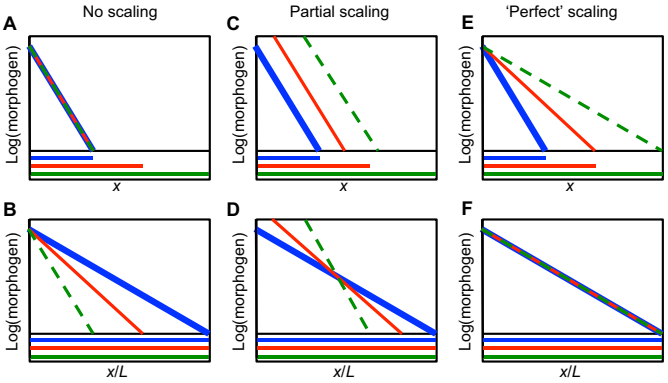

Fig. 2. Schematic profiles showing examples of morphogen distributions that exhibit different degrees of scale invariance. (A-F) Graphs showing the distribution of morphogen on an absolute positional scale (A,C,E) and on a normalized position scale (B,D,E) in short (blue), medium (red) and long (green) domains. The overall system length is L and x is the coordinate. Line colors for the morphogen in the plots correspond to the same colored domain length. Line thicknesses vary so they can be distinguished where they overlap. Examples of no scaling (A,B), partial scaling (C,D) and perfect scaling (E,F) are shown.

How specific transport processes and kinetics are incorporated into the continuity equation

The continuity equation (Eqn 1) is universally true and applies to all transport mechanisms equally (Fig. 4), but to proceed, one must specify the details of the transport and kinetic processes involved. The description of transport depends on the mechanisms involved (Fig. 4A-F), which can include advection, active transport (Fig. 4D,E), and diffusion with or without geometric barriers (Fig. 4A,B). The expression of the dependence of the flux on the characteristics of the local morphogen field and other factors that contribute to the flux is called a constitutive equation (see Glossary, Box 1), and these are usually empirical statements that reflect experimental observations, but sometimes they can be derived from first principles.

How to describe a transport process may depend on the time and space scales of the observations. Transport processes that contain a random component, such as the run-and-tumble movement of bacteria, can often be described as a diffusion process on appropriate time and space scales (Hillen and Othmer, 2002). For such processes, the flux of species i takes the familiar form of Fick's law of diffusion (see Glossary, Box 1), which is:

$$j_{i,x} = -D_i \frac{\partial c_i}{\partial x} \,, \qquad (2)$$

wherein D_i is the diffusion coefficient of species i.

Anisotropic transport can arise if a molecule is carried along microtubules by a motor molecule, for if the microtubules are aligned the transport will be highly directional, as in neuronal transport. However, if the dwell time of the cargo on the microtubule is relatively short and the microtubules are randomly oriented, the new direction of the motor and cargo after re-binding is chosen randomly, and when viewed over a long time scale and over a sufficiently large spatial scale the transport process can also be described as diffusive (Fig. 4E) (Hillen and Othmer, 2002). Other types of anisotropic fluxes arise from directed motion, due, for example, to tissue growth, to fluid flow, to drift in the diffusion process, or to active transport. The simplest flux relations for these have the general form $\mathbf{j}_i = \mathbf{v}c_i$, where $\mathbf{v}$ is now a macroscopic velocity. A more general form that may be applicable to signal transport along cytonemes (Roy et al., 2011),

Development (2013) doi:10.1242/dev.100511

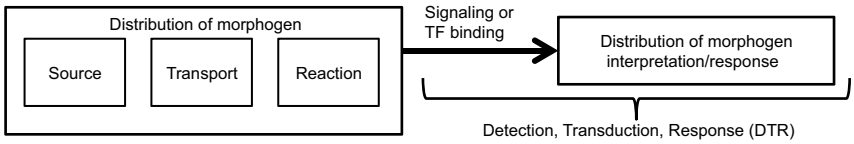

Fig. 3. Modules involved in patterning systems. Patterning systems typically comprise four interacting modules: (1) a source module that generates the morphogen signal; (2) a transport module for communicating the signal; (3) a reaction module that interacts with modules 1 and 2 to regulate morphogen gradient shape; and (4) a module for detection and transduction of the signal, interpretation of the transduced signal, and initiation of a response (the DTR module).

which are specialized signaling filopdia of varying length, arises when the flux at a point is a suitably weighted average of the concentration field in a neighborhood of the point.

In general, there will be more than one species in a patterning model, and some, such as receptors, may remain localized in space. In one space dimension this leads to the system of equations:

$$\frac{\partial c}{\partial t} = -\frac{\partial j_x}{\partial x} + R(c,s,p)\,, \tag{3}$$

$$\frac{\partial s}{\partial t} = S(c,s,p)\,, \tag{4}$$

wherein $c=(c_1, c_2, \ldots, c_n)$ represents the concentrations of all mobile species, j_x is the vector of fluxes of the species, and $s=(s_1, s_2, \ldots, s_m)$ represents all immobile species. The functions R and S encode all the kinetic steps that lead to changes in the mobile and stationary species, respectively, and we have explicitly incorporated the vector p of parameters, which includes rate constants and other parameters, in these functions. The details of how the use of this flux relation leads to a general form of reaction-diffusion advection equations for the spatiotemporal evolution of the concentration of morphogens and other species are given in supplementary material Box S1 in Appendix S1.

Scaling properties of reaction-diffusion models

To illustrate how patterns scale when transport is by diffusion only, and how the system can be modified to lead to scale-invariant patterning, we discuss a simple example. Consider a one-dimensional system of length L in which the morphogen, of concentration m, is injected or produced at the left boundary at a rate q, diffuses throughout the domain, and undergoes first-order decay at a rate k_m. The governing reaction-diffusion equation for m is

$$\frac{\partial m}{\partial t} = D_m \frac{\partial^2 m}{\partial x^2} - k_m m\,. \tag{5}$$

Further details are given in supplementary material Box S2 in Appendix S1, where boundary and initial conditions are explicitly given. If we scale the space variable by setting $\xi=x/L$, then $\xi \in [0, 1]$, and this equation becomes

$$\frac{\partial m}{\partial t} = \frac{D_m}{L^2} \frac{\partial^2 m}{\partial \xi^2} - k_m m\,. \tag{6}$$

Because all terms in this equation have the units of concentration/time, we can see that there are two characteristic time scales that govern the dynamics: the diffusion time scale $t_D \equiv L^2/D_m$, and the reaction time scale $t_R \equiv 1/km$ set by the lifetime of the morphogen. As a system increases in length, the time scale for

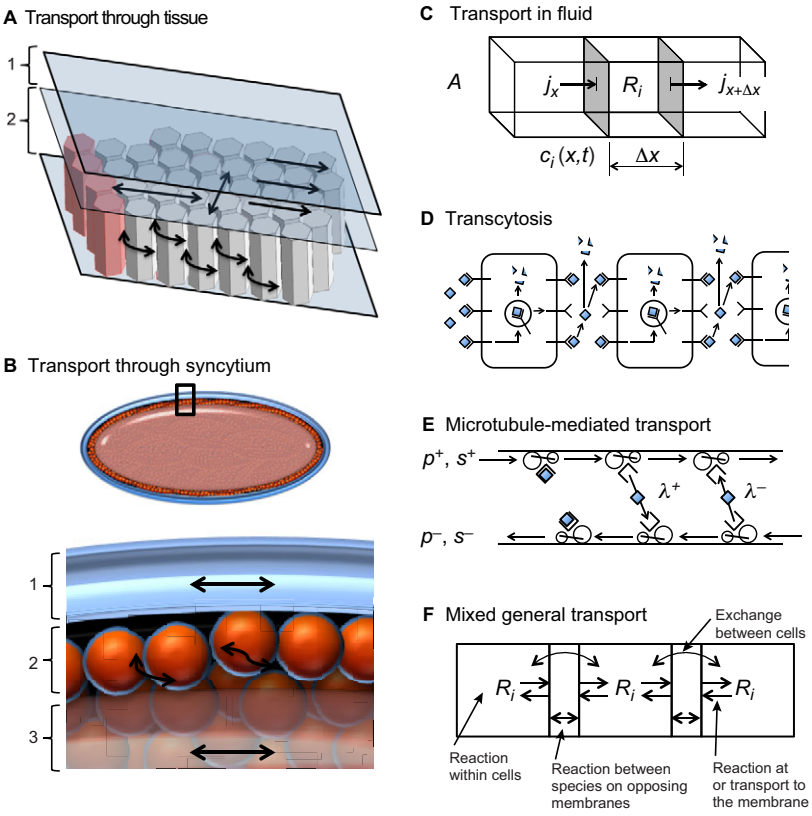

Fig. 4. Morphogen transport mechanisms. (A) Example cutaway view of transport through an epithelial layer similar to the wing imaginal disc. The lumenal layer (1) and columnar epithelial cell layer (2) present different obstacles to transport. Arrows indicate free diffusion in the lumen and hindered diffusion between cells in the epithelial cell layer. (B) Transport through the *Drosophila* blastoderm embryo depends on spatial location and can occur relatively freely through the perivitelline space (1) and through the cortical cytoplasm (2) prior to cellularization. Transport through the yolk (3) may be hindered by higher viscosity, which slows transport. (C-F) Biophysical aspects of transport. (C) General contributions to the amount of a morphogen in a small volume of fluid by flux in and out of the volume and reactions within the volume. Here, j is the flux, R_i is the reaction term, c_i is the concentration, A is the cross-sectional area and Δx is the length interval. (D) Cell-mediated transport or transcytosis mechanism (Bollenbach et al., 2005; Kruse et al., 2004). (E) Transport mediated by microtubule motors may provide directed transport or diffusive transport depending on the binding parameters of a molecule to the motor proteins (Hillen and Othmer, 2002; Dou et al., 2012). p^+ (p^-) is the particle density moving to the right (left); s^+ (s^-) is the speed of particles moving to the right (left); and λ^+ (λ^-) is the probability of a particle moving to the right (left) changing direction and beginning to move left (right). (F) A mixed or general transport model that integrates the concepts shown in C-E and other forms of molecular motion and reaction.

Development (2013) doi:10.1242/dev.100511

transport by diffusion increases in proportion to the length squared, whereas the kinetic time scale is unaffected by changes in length. Thus, we can already predict that to obtain a scale-invariant morphogen distribution we must either speed up diffusion or slow down the reaction rate appropriately; this is true in general, even if the kinetic mechanism involves bimolecular steps (Othmer and Pate, 1980). However, we must also consider the input flux (q) of morphogen, and if this is done we find that with some simplifications (supplementary material Box S3 in Appendix S1), the spatial distribution of the morphogen at steady state is:

$$m(\xi) = m\left(\frac{x}{L}\right) \approx \frac{q}{\sqrt{k_m D_m}} \exp\left(-\sqrt{\frac{k_m L^2}{D_m}}\xi\right) = A_m \exp\left(-\lambda\left(\frac{x}{L}\right)\right). \quad (7)$$

From this, we can see that the quantity $k_m L^2/D_m \equiv \lambda$ determines how rapidly the profile decays in space and that either slow diffusion or rapid decay leads to rapid spatial decay of m.

As shown in Fig. 2, determining whether a morphogen profile is scale invariant is easy when the distribution is plotted versus the scaled position, but it is also readily apparent by inspection of Eqn 7. There are two dimensionless groups in this equation: the quantity A_m that represents the maximum amplitude of the distribution [which occurs at the input (ξ=0)], and the quantity λ that controls the spatial distribution of the morphogen via the exponential factor. These two dimensionless groups in turn depend on the parameters D, k, q and L, which characterize the diffusion, reaction, and input processes and the length of the system. If the length L of the system increases at fixed values of D, k and q, the profile will decay more rapidly relative to the system size and the pattern would be compressed towards the left (Fig. 2A,B). If these parameters vary with the length, then different degrees of scale invariance can be achieved by varying these parameters appropriately. An analysis of the various possibilities is given in supplementary material Boxes S2-S5 in Appendix S1. The essential ideas that emerge from the analysis can be described as follows.

To achieve scale invariance throughout the domain, both A_m and λ must be independent of L, and this can be achieved in a variety of ways. If each of the parameters D, k and q vary with L according to a power law relation as given in Eqn 1 (e.g. $D=D_0 L^a$) where a is the power, one can establish all possible ways of parameter variation that lead to global scale invariance. Examples of specific choices for the scalings are given in Table 1. For example, if we suppose that the input flux is fixed, then the only mechanism that achieves scaling of amplitude and shape is one that increases the rate of diffusion in proportion to length and decreases the reaction rates by an amount directly proportional to length (Fig. 5A,E). This provides the ideal situation in which the range is extended for increases in system length, without altering the peak levels of morphogen. If only one of diffusion or reaction rate is modulated, the amplitude is not constant and increases if scaling is achieved by reducing the morphogen decay rate in linear models (Fig. 5B,E) or decreases if scaling is achieved by increasing the rate of diffusion (Fig. 5C,E). The corresponding amplitudes are shown in Fig. 5D. Of course, if the flux (see Glossary, Box 1) is adjusted accordingly, perfect scale invariance can be achieved. It should be noted that modulation of the diffusion coefficient or the input flux does not affect the time scale for the evolution of the spatial profile (supplementary material Box S2 in Appendix S1; Table 1), whereas modulation of the reaction time scale does, and the latter may limit the applicability of this strategy in rapidly developing systems such as the *Drosophila* embryo.

If the objective is to establish a threshold of morphogen at a fixed relative position in the system, one solution would be to simply increase the morphogen supply rate q to the system (Fig. 2C,D) in order to offset the faster relative decay that results from holding D and k constant. However, this only achieves exact invariance at one point, and the morphogen distribution on either side of that point would not be scale invariant; all positions to the left or right of the balance point would be either hypo- or hyper-scaled (Fig. 5E) relative to the original shape. This mechanism, which we refer to as 'flux-optimization', is analyzed further in supplementary material Box S5 in Appendix S1.

A system in which several transport mechanisms contribute to the flux is analyzed in supplementary material Box S3 in Appendix S1. To achieve scale invariance when both advection and diffusion contribute to the morphogen distribution, it is necessary to modulate the convective flux in addition to the modulation described above. If diffusion is constant and both diffusion and advection are of the same order of magnitude, the morphogen profile cannot scale in general, with the exception of one scenario in which the velocity for convection decreases in proportion to the inverse of the system size. This could be true, for instance, if the area growth rate of a tissue is constant in time. However, advection can be neglected in most currently investigated systems, leaving only diffusion and reaction as the contributing processes.

Finally, although the above discussion is presented for a single species, it applies equally well to systems containing other species in the patterning scheme, but now one must identify a scaling factor for all diffusion coefficients and a single factor for all reactions, if the pattern of all species is to be scale invariant. Thus, although the requirements on D, k, and q for scale invariance are relatively straightforward, two very important questions remain. First, what mechanisms could confer the necessary regulation of D, k, and q to produce scale invariance? And, second, how is scaling achieved in actual morphogen patterning systems?

Control of the pattern scale by 'size-sensor' molecules: passive and active modulation

We now know the mathematical requirements for scaling based on how diffusion and reaction terms must be modified in general, and have analyzed the requirements for systems with diffusion and linear decay. Next, we describe hypothetical mechanisms for accomplishing the scaling by introducing a modulator M that regulates the reaction and transport characteristics of the morphogen (Fig. 6A). We return to the general example discussed previously,

Table 1. Modes of modulation that lead to scale invariance for diffusion-decay models (Eqn 7).

Modulated property			Impact			
k_m	D_m	q	Patterning time	Peak $q/\sqrt{k_m D_m}$	Range $\sqrt{k_m L_2/D_m}$	Requirement of input flux for scaling
$\downarrow\propto L^{-2}$	–	–	$\uparrow\propto L^2$	$\uparrow\propto L$	Scaled	$\downarrow\propto L^{-1}$
–	$\uparrow\propto L^2$	–	No change	$\downarrow\propto L^{-1}$	Scaled	$\uparrow\propto L$
$\downarrow\propto L^{-1}$	$\uparrow\propto L$	–	$\uparrow\propto L$	No change	Scaled	No change
–	–	$\uparrow$	No change	$\uparrow$	Not scaled	–

Development (2013) doi:10.1242/dev.100511

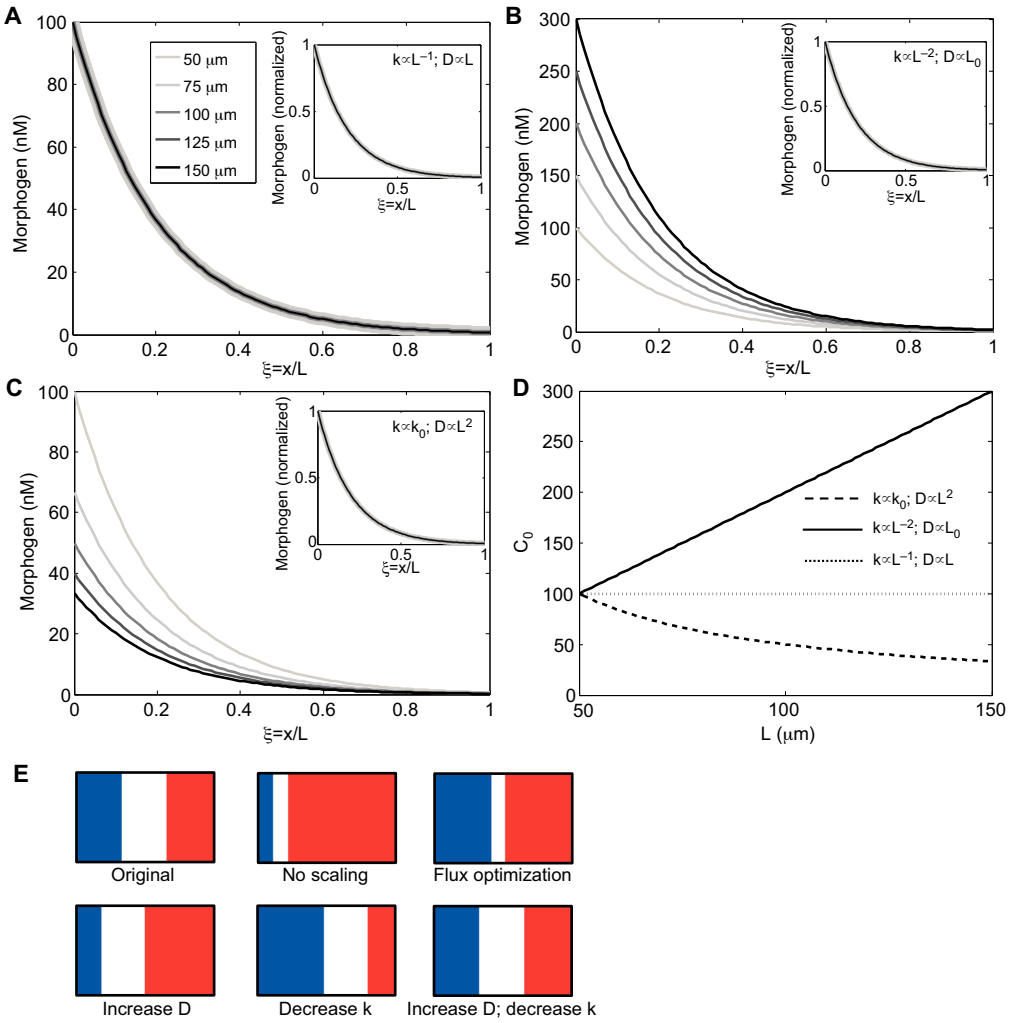

Fig. 5. Impact of modulating diffusion and decay for linear morphogen decay models. (A-D) Plots of the distributions that result from numerical solution to Eqn 7 are shown. Insets in A-C show distributions for amplitude-normalized profiles. (A) Scaling achieved by simultaneous targeting of diffusion and reaction leads to shape and amplitude scaling without further modification of input flux. (B) Decreasing decay rates in proportion to L^2 achieves scaling of the normalized profile (inset), but this leads to an increasing amplitude without a balanced decrease in morphogen input flux. (C) Increasing the diffusion in proportion to L^2 results in decreasing amplitudes without a balanced increase in morphogen flux. (D) Summary of changes in maximum concentration in A, B and C. (E) Examples of how the morphogen distributions that arise from the different mechanisms in A, B and C are reflected in the patterning for the French flag paradigm. D, diffusion coefficient; k, decay rate; L, system length.

and now require two equations: one (Eqn 8) is the new form of the equation for morphogen transport that includes modulation of diffusion and reaction terms by M, and one (Eqn 9) provides the balance equation for the modulator M, the diffusion coefficient of which is D_M and which may or may not be regulated by the morphogen in the system:

$$\frac{\partial m}{\partial t} = \frac{\partial}{\partial x}\left(D_m(M)\frac{\partial m}{\partial x}\right) + k_m R_m(m, M)\,, \qquad (8)$$

$$\frac{\partial M}{\partial t} = D_M \frac{\partial^2 M}{\partial x^2} + R_m(m, M)\,. \qquad (9)$$

The boundary conditions on the morphogen are as before, and the boundary conditions on the modulator M are specific to a particular mechanism; examples are given later and in supplementary material Box S4 in Appendix S1.

The possible interactions between the morphogen and the modulator in this '*m&M*' mechanism are shown in Fig. 6A. As written, the morphogen and modulator interact in a reciprocal manner, in that the reaction rate R_m depends on the modulator M, and the reaction rate R_M (m, M) may depend on m. The first case to be considered arises when the modulator kinetics R_M (m, M) are independent of the morphogen, and we call these passive mechanisms. In this case, the blue lines in Fig. 6A are absent. By contrast, when morphogen and modulator are tightly coupled, we refer to this as an active mechanism. Passive mechanisms have the advantage that the modulator can be used in successive steps of patterning, even on a global organismic level, whereas in an active mechanism the morphogen and modulator dynamics are tightly linked. However, an active mechanism has the advantage of being able to adjust the levels of modulator throughout patterning.

In either case, modulators can be used to adjust the characteristic time scales of diffusion and/or reaction in a size-dependent manner in order to achieve the proper proportions of morphogen patterning. Modulation of the reaction rates can involve a modulator that acts either as a catalyst to enhance the rate of reactions or as an inhibitor that retards a reaction. For instance, if the modulator acts to increase a reaction rate, then scaling can be achieved if the concentration of the modulator decreases in correct proportion to the tissue size. If the modulator acts to slow a reaction, an increase in the level of the modulator can lead to the appropriate level of scaling (supplementary material Box S4 in Appendix S1). The modulator can also act by enhancing or slowing diffusion, and thus there are many theoretically possible mechanisms that lead to appropriate scaling. There is, however, one essential difference between the morphogen and the modulators in a patterning system that scales correctly. Whereas the amplitude and shape of the morphogen distribution is size invariant, the level and perhaps the spatial distribution of the modulator is not; in effect, the modulator level must reflect the system size, and rises or falls accordingly (supplementary material Box S4 in Appendix S1). This is the

Development (2013) doi:10.1242/dev.100511

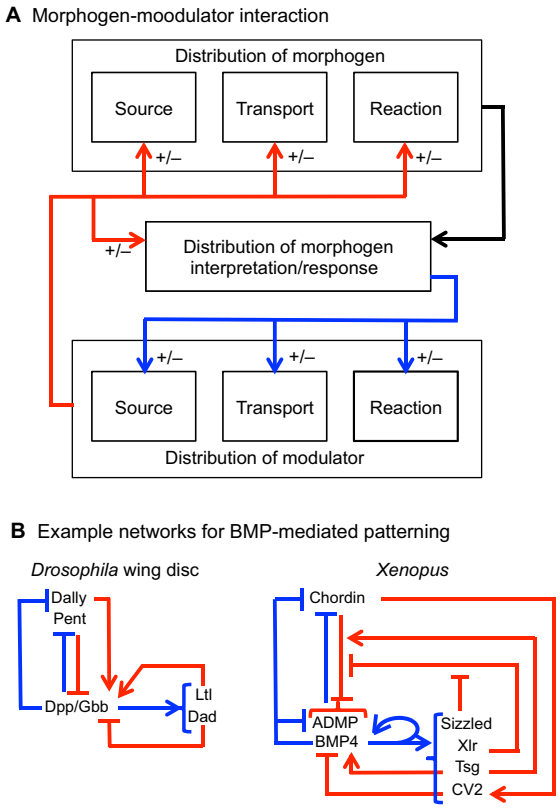

Fig. 6. Potential interactions between the source/transport/response components and the modulator species. (A) Modulator-mediated control of morphogen distribution and interpretation is shown by red lines. Control of the modulator by the morphogen is indicated by blue lines. (B) Examples of networks for BMP-mediated patterning. The network on the left shows the connections between the morphogens Dpp/Gbb, the extracellular modulators Dally and Pent, and the molecules that impact morphogen interpretation/response (Ltl/Dad) during BMP-mediated patterning of the *Drosophila* wing disc. The network on the right shows the connections between morphogens (BMP4, ADMP), and extracellular modulators (Sizzled, Xlr, Tsg, CV2 and Chordin) during dorsal/ventral patterning of *Xenopus* embryos.

principal trade-off in the modulator scheme: any gain in scaling in the morphogen of interest can only be achieved by another factor that reflects the length information in its distribution. In essence, the modulator distribution encodes the system size and the patterning mechanism can use this information to adjust relevant rates accordingly.

As passive scaling mechanisms involve no feedback from the morphogen dynamics (Fig. 6, red lines only), we can analyze a variety of mechanisms that can be coupled with particular morphogen patterning systems. In the first type, we suppose that the modulator is produced in a restricted region of the domain in which patterning occurs, for instance by production at a boundary of the domain or by a specialized group of cells in the interior. In addition, it diffuses throughout the system and decays via a first-order reaction. If the total production of this modulator is independent of the system size, because, for example, the number of secreting cells does not change with the size of the domain, then the average concentration of the modulator scales in proportion to the size of the system, i.e. $M_{avg} \propto 1/L^P$, where P=1, 2, 3 is the dimension of the underlying spatial domain. If, in addition, the modulator diffuses rapidly on the time scale of patterning, then uniform modulation of reaction and/or transport characteristics is possible, and scale invariance can be ensured. If it is not uniform in space, the modulation will not be uniform, but the scaling may still occur at spatial locations where it is needed.

Active modulation arises when morphogen distribution affects the formation, and therefore the spatial distribution, of the modulator. Examples of active modulator mechanisms include the expander repressor feedback motif (Ben-Zvi and Barkai, 2010; Ben-Zvi et al., 2011) and other examples in which feedback between multiple modulator species or multiple morphogens modulate the reaction and transport rates to produce proper scaling. The desired outcome of active modulation is the scaling of diffusion and/or reactions as before, but in active modulation, feedback on the modulator dynamics provides a dynamic regulation of the biophysical parameters to achieve the desired scaling of components.

Systems that scale

Through the mathematical analysis above, we have now identified three generic mechanisms that can produce scale invariance: (1) flux optimization; (2) active modulation of reaction or transport parameters; and (3) passive modulation of reaction or transport parameters. In the section below, we discuss biological examples of these mechanisms in detail.

Potential examples of flux optimization: scaling of the anterior-posterior Bicoid pattern in *Drosophila* embryos

In the developing *Drosophila* embryo, translation of maternal *bicoid* (*bcd*) mRNA that is distributed in a short-range gradient originating at the anterior end produces Bicoid (Bcd) protein, which diffuses throughout the embryo (Little et al., 2011). This leads to an anterior-posterior (AP) gradient of Bcd that establishes polarity of the embryo and serves as the first step in a patterning hierarchy that culminates in expression of the segment polarity genes. At the same time, nuclei in the embryo undergo 13 cycles of synchronous division, and during cycle 10 translocate from the core to the cortex, where they remain for the next rounds of nuclear division. During cycle 14, there are ~6000 nuclei localized at the embryonic cortex, and at this stage membranes form and segregate the syncytial nuclei into individual cells (Foe and Alberts, 1983).

It is found experimentally that the Bcd distribution is approximately exponential (Fig. 1A), which, as can be seen in Eqn 7 and in supplementary material Box S3 in Appendix S1, could arise from the interplay between diffusion and first-order decay (Houchmandzadeh et al., 2002; Gregor et al., 2005). The Bcd level initiates the expression of the downstream gap genes, which include *hunchback*, *Kruppel*, *knirps* and others, in circumferential strips transverse to the AP axis (reviewed by Jaeger, 2011). However, owing to cross-regulation between the gap genes themselves, the interpretation of Bcd input by the gap gene network is not a simple threshold response, which may allow for greater levels of variability in the Bcd input than would be tolerated by other mechanisms. Intriguingly, the degree and mode of Bcd scale invariance is different depending on whether the comparison is between species of the same genus (interspecies) or within the same species (intraspecies).

A comparison of the Bcd distributions between closely related Dipterans (see Glossary, Box 1) that utilize Bcd for AP patterning showed that the spatial distribution of Bcd scales in direct proportion to the size of the embryo (Gregor et al., 2005). Although the related dipteran species varied in size, from ~344 μm (*Drosophila busckii*) to ~1420 μm (*Lucilia sericata*), the profiles of Bcd protein staining appear to expand in direct proportion to the length of the embryo (Fig. 1A). When rescaled to normalized coordinates (either percent embryo length, or equivalently $\xi = x/L$) the interspecies variation of

Development (2013) doi:10.1242/dev.100511

the profiles is no larger than the intraspecies variations, and thus the relative positions of target gene expression patterns are unchanged.

An early suggestion to account for this interspecies scaling of the Bicoid gradient was based on the observation that the total number of nuclei between species that differed by approximately fivefold in length was nearly constant, because they undergo the same number of division cycles (Gregor et al., 2005). As nuclei in the dipteran species studied are localized at the embryonic cortex, one possibility was that nuclei play a role in the modulation of Bcd decay (Gregor et al., 2005; Gregor et al., 2007; Umulis, 2009; Miles et al., 2011). If the decay rate is proportional to nuclear density, if the number of nuclei remains constant, and if transport is limited to the embryonic cortex, then scaling of the gradient naturally emerges as a property of the patterning system (Umulis et al., 2008; Gregor et al., 2007; Umulis, 2009). This is easily understood by reference to the rubber sheet analogy. If the nuclei controlled morphogen decay, the increased density of nuclei in shorter species would lead to a dynamic shortening of the intrinsic Bcd length scale. However, a role for nuclei as a mediator of scaling, either within or between species, conflicts with measurements of the gradient during cycles 10-14, which appears to be temporally and spatially invariant, even though the number of nuclei increases 16-fold (Gregor et al., 2007; Grimm et al., 2010; Grimm and Wieschaus, 2010; Miles et al., 2011; Coppey et al., 2007). Another possibility that has been considered is that evolution has acted on the lifetime of Bcd molecules in each species, which leads to a broader range in larger embryos with more stable Bcd molecules, or a shorter range in smaller embryos with less stable Bcd molecules (Gregor et al., 2008). Intriguingly, it was found that the molecular lifetime is not an intrinsic property of species-specific Bicoid protein. Instead, it appears to be mediated by the embryonic environment or machinery that regulates the distribution of Bcd, presumably by altering transport or decay rates (Gregor et al., 2008).

By contrast, intraspecies scaling of Bcd patterns appears to rely on a completely different mechanism than interspecies scaling. Recently, Cheung et al. (Cheung et al., 2011) investigated Bcd patterning between artificially selected populations of an initially wild-type *Drosophila melanogaster*. After successive rounds of selection, two populations were developed that differed in egg length by ~25%. Small embryos with a length of ~518 μm and large embryos with a length of ~645 μm yielded Bcd patterns that had the same intrinsic length scale for Bcd variation. As the intrinsic scale is not changed, perfect invariance is not possible, but approximate scaling could result from modulation of the amplitude of the gradient. A hint of an alternative mechanism emerged from careful quantification of the Bcd distributions in populations of large and small embryos, which showed that the maximum value of the Bcd distribution increased by ~66.9%, a number that correlated with an embryo volume difference of 71.7%, thus suggesting volume-dependent scaling.

An alternative interpretation of the volume-dependent production of Bicoid scaling is that the input flux is optimized to the levels needed for adequate scaling (Umulis and Othmer, 2013). Solution of Eqn 7 with input flux optimization produces profiles that provide adequate, but not perfect, scaling of Bicoid (Fig. 7A,B). These profiles are further corrected by canalization of the gap gene patterning network as it evolves to form stable patterns of gene expression (Fig. 7C) (Jaeger et al., 2007; Bergmann et al., 2007; Lott et al., 2007; Manu et al., 2009; Hengenius et al., 2011). The analysis in supplementary material Box S5 in Appendix S1 summarizes how flux optimization can lead to increases or decreases in amplitude that provide 'enough' scaling to meet the performance objectives of development in systems that do not modulate the intrinsic scale, and this may suffice for relatively small increases and decreases in length. If patterning occurs by interpretation at only one threshold concentration, an increase or decrease in the source strength q can lead to the same concentration at the same relative spatial location. However, many morphogens regulate multiple targets that respond to different levels, and hence different spatial locations or histories of exposure to the morphogen.

Examples of passive modulation

Although the role of nuclei in regulating the distribution of Bcd is not clear, a nuclear density-based mechanism might play a role in the scaling of other patterning steps in the embryo and may hence act as a form of passive modulation of morphogen parameters. For example, the distribution of dpERK (the phosphorylated form of extracellular-signal related kinase), which is known to pattern terminal regions of the *Drosophila* embryo in response to spatial activation of the Torso receptor, has peaks at the anterior and posterior poles of the embryo that refine during nuclear cycles 10-14 in direct proportion to nuclear density (Coppey et al., 2008). Another scenario in which modulation of a morphogen gradient is

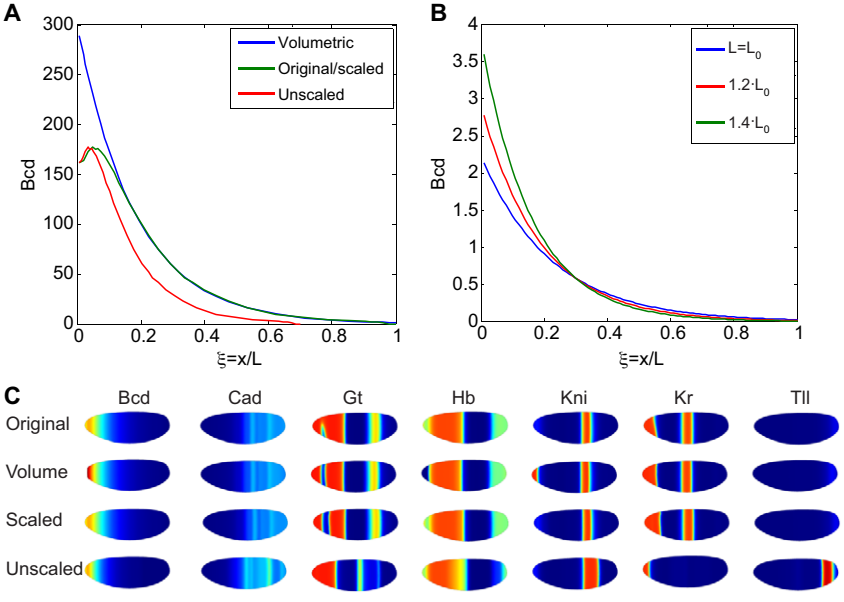

Fig. 7. Scaling of the Bcd gradient by adjustment of morphogen range or by volume-dependent production of Bcd. (A) Predicted relative Bcd levels along the AP axis of *Drosophila* embryos for a volume-dependent production mechanism (blue), a hypothetical perfect scaling mechanism (green) and for no scaling (red) of Bcd. Bcd levels in the original-sized (i.e. base) embryos is shown in green. (B) Predicted Bcd distributions under the flux optimization hypothesis. The individual distributions intersect at x/L=0.3, which is the local region that provides the best scaling. (C) Predicted expression boundaries for the gap genes downstream of the Bcd input shown in A using the models by Hengenius et al. (Hengenius et al., 2011). Spatial patterns of gene expression for original, volume-dependent increase in Bcd, and perfectly scaled Bcd show very similar spatial patterns. Unscaled Bcd predicts dramatic shifts in gap gene expression boundaries.

achieved by targeting nuclear density is patterning by the transcription factor Dorsal (Chahda et al., 2013). Dorsal establishes a ventral-to-dorsal high-to-low gradient in the embryo, accumulates in cortical nuclei, and dynamically evolves during cycle 10-14 of embryogenesis (Crocker et al., 2008; Mizutani and Sousa-Neves, 2010). Although evolution has selected for Dorsal distributions that are not perfectly scaled between related *Drosopholids*, the shape of the distribution is affected by the size and density of nuclei, which augments the pattern adjustments made by the upstream cascade that localizes Dorsal nuclear accumulation.

How modulator mechanisms can evolve in contexts in which proper levels of the modulator are not achieved automatically, either owing to fluctuations in the number of secreting cells or their production rates, is another issue. A modulator that acts as a catalyst to enhance binding or other reaction rates can be optimized for proper levels of expression on an evolutionary time scale. Because the modulator can modify either diffusion or any reaction scheme, it can be tuned to provide scaling in different species of the same patterning pathway or provide a means for rapid evolutionary divergence of a morphogen pattern to achieve different performance objectives in response to selection pressures. We speculate that such modulators may exist for Bcd patterning and for Decapentaplegic (Dpp) patterning along the dorsal surface of blastoderm embryos (Fig. 1A-C), although they remain to be characterized. Furthermore, the mechanisms for such passive scaling extend beyond regulation of binding site density and include other patterning regulators that can affect the range of morphogen (Umulis et al., 2008; Umulis et al., 2010). A number of candidate molecules with the capacity for global regulation exist, although they have not yet been investigated in regards to their role in scale invariance. For example, the bone morphogenetic protein (BMP) regulator Twisted gastrulation (Tsg) regulates numerous processes simultaneously, including the binding of Sog to Dpp (impact on k_m), and the processing rate of Sog-Tsg complexes by the metalloprotease Tld (impact on k_m), and has been suggested to have a Sog-independent role in recruiting Dpp to the embryonic surface, presumably by interaction with receptors (impact on D_m) (Shimmi et al., 2005; Wang and Ferguson, 2005). Because Tsg impacts so many processes that regulate shape, amplitude and dynamics simultaneously, it is a natural candidate to adjust the entire system appropriately to achieve scaling from a biophysical perspective.

Examples of active modulation: the *Drosophila* Dpp gradient

In the *Drosophila* wing imaginal disc, the BMP ligands decapentaplegic (Dpp) and glass bottom boat (Gbb) produce a gradient of signaling and gene expression activity along the anterior-posterior axis of the disc. The *dpp* gene is expressed in medial cells between the anterior and posterior compartments and establishes a long-range, nearly exponential, distribution in the posterior compartment (Fig. 1D). The activity gradient sets the pattern of longitudinal veins, and is involved in the regulation of tissue growth. It has been found experimentally that the gradient of Dpp does not scale perfectly when assayed by measurement of the gradient of a Dpp-GFP fusion protein (Wartlick et al., 2011). The morphogen range scales in proportion to disc size and, as a result, when concentrations are normalized by peak intensity, the profiles are essentially size independent (Fig. 2D) (Wartlick et al., 2011). The amplitude of Dpp-GFP increases with time as the disc grows, and the increase correlates strongly with cell growth and division rates in the growing wing disc (Wartlick et al., 2011).

A number of secreted species regulate the BMP activity gradient, including the glypican Dally, Larval translucida (Ltl), and Pentagone (Pent) (Vuilleumier et al., 2010). *pent* is the name used for gene CG2264 in the primary literature describing scale invariance of developing wing primordia referenced herein (Vuilleumier, et al., 2010; Ben-Zvi et al., 2011; Hamaratoglu et al., 2011). It is now known as *magu* (Li and Tower, 2009). Ltl, together with the intracellular inhibitory smad protein Dad, is upregulated by BMP signaling, whereas *pent*, *dally* and the BMP receptor gene *thickveins* (*tkv*) are downregulated in response to BMP signaling (Fig. 6A). In addition, Ltl interacts with Dally and appears to exhibit biphasic regulation of BMP signaling. Loss of *pent* results in contraction of the pMad gradient (which provides a readout for BMP signaling), an increase in pMad amplitude (Vuilleumier et al., 2010), and a greater loss of Dpp-HA in pulse-chase experiments (Vuilleumier et al., 2010), all consistent with Pent activity acting on the Dpp lifetime, a process that would regulate the range of Dpp activity. Pent also interacts with Dally, presumably to modify the access of Dpp to its receptors, and, like *dally* expression, *pent* expression is repressed by Dpp signaling. Recently, it was found that loss or ectopic overexpression of *pent* reduces scaling of the activity gradient and the distribution of downstream target genes in wing discs (Hamaratoglu et al., 2011; Ben-Zvi et al., 2011).

An active modulation mechanism based on Dpp, Tkv, Pent and Dally has been proposed to explain the observed scaling of the Dpp distribution in the *Drosophila* wing disc (Ben-Zvi et al., 2011). The model is an extension of an earlier expander-repressor (ER) scheme (Ben-Zvi and Barkai, 2010) in which the ‘expander’ functions to either speed up diffusion or slow reactions, and is under negative control of the morphogen. In the model of the wing disc, the primary morphogen is Dpp, whereas Dally and Pent serve as modulators, affecting both the diffusion coefficient of Dpp and the on-rate of Dpp to Tkv to different extents depending on the hypothesized primary molecular function of Pent. The structure of the model [see equation S2 in Ben-Zvi et al. (Ben-Zvi et al., 2011)] is formally equivalent to that given in supplementary material Box S1 in Appendix S1 and in Eqns 8-9, but the equations lack the term in Eqn 8 and Eqn 9 that accounts for the spatial dependence of the diffusion coefficient through its dependence on modulators. The complete model comprises six equations with 27 parameters, and we refer the reader to Ben-Zvi et al. (Ben-Zvi et al., 2011) for details. In the model, Pent interacts with Dally and the combination of Dally and Dally-Pent increase the diffusion coefficient and decrease the rate of Dpp-Tkv binding (which leads to endocytosis and ligand destruction) (Fig. 8A). Under the assumption of a uniform spatial distribution of Pent, the ER mechanism produces good scaling of the morphogen distribution with normalized concentration (compare Fig. 1D with Fig. 8B) as reported (Ben-Zvi et al., 2011). However, the amplitude of the morphogen-receptor complex decreases more than twofold for a twofold increase in length (Fig. 8C), suggesting that this mechanism alone cannot account for the observed amplitude increases in the distribution and activity of Dpp-GFP. As a result, the overall effect is that the Dpp distribution is not scale invariant, even if Pent diffuses very rapidly. The same requirements for proper flux regulation are present in the ER mechanism as discussed earlier for linear morphogen decay models: decreases in the effective decay rate by expander(s) can lead to increased amplitude of the morphogen distribution, whereas if the expander increases the diffusion coefficient this leads to a decrease in morphogen amplitude. Thus, although the ER mechanism is much more complex than the simple linear decay model, it appears that the effect of modulation of the diffusion coefficient dominates, thereby producing a decrease in amplitude. The underlying ER mechanism presents an example of active, feedback-driven modulation to adjust the morphogen range for changes in the size of the domain. However,

Development (2013) doi:10.1242/dev.100511

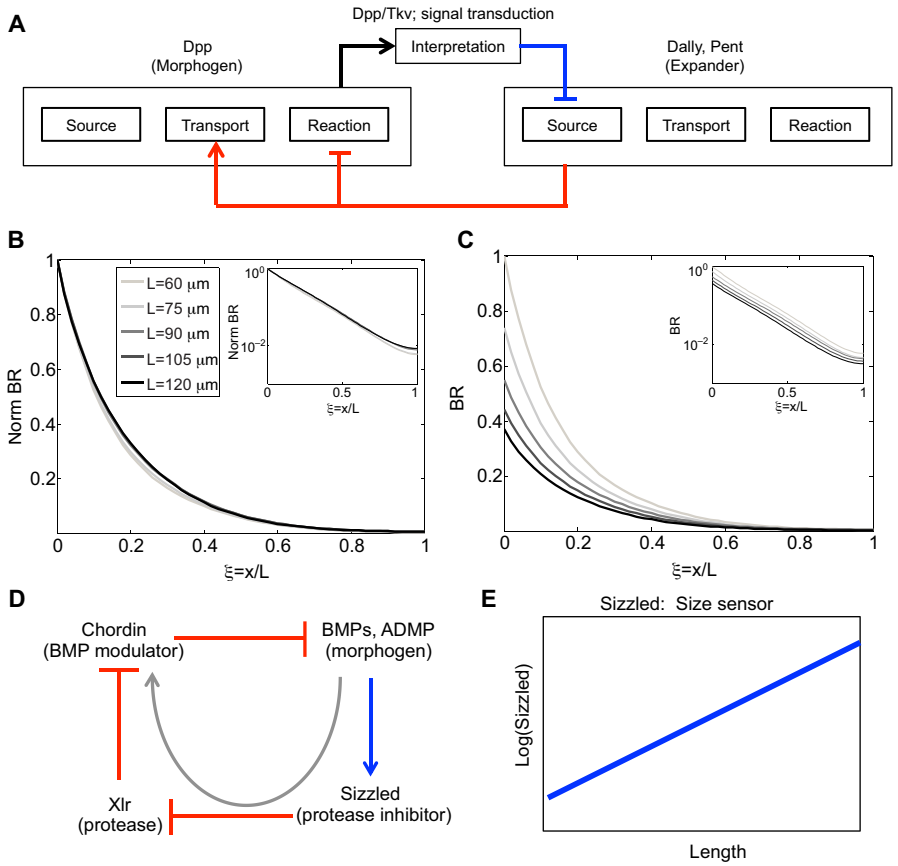

Fig. 8. Pentagone- and Dally-mediated regulation of Dpp signaling produces active scaling by an ER feedback mechanism. (A) Schematic showing expander-repressor regulation of modulator action on the morphogen Dpp. Expander corresponds to Dally and Pent that feeds back (red lines) to modify the reaction and transport properties of the morphogen Dpp, which subsequently represses the expander (blue line). (B) Predicted distribution of normalized Dpp-Tkv (BR) as a function of relative position in different size discs that range from 60 to 120 μm. Here, the expander-repressor motif correctly adjusts decay length to provide scale invariance during disc growth. Inset shows log scale. (C) Same as in B except all individual profiles are normalized to the amplitude in the 60-μm disc. (In B, each profile is normalized to itself, which leads to each having a maximum amplitude of 1.) The plot shows decreasing morphogen amplitude as a function of disc size and developmental time. Inset shows log scale. Parameters and equations are provided in Ben-Zvi et al. (Ben-Zvi et al., 2011). (D) Core feedback scaling network in the 'size-sensor' model (Inomata et al., 2013). Here, feedback from BMP signaling (blue line) works through the modulators (red lines) Sizzled and Xlr to enhance the function of Chordin, which sequesters extracellular BMPs (a negative regulation). The gray arrow shows the net impact of feedback from BMP signaling on Chordin. (E) Proposed behavior for Sizzled in relation to embryo size according to the 'size-sensor' model (Inomata et al., 2013).

the mechanism cannot automatically account for the changes in amplitude that are also observed as the disc grows. This suggests that other factors are determining the amount of input flux of Dpp, or other feedback mechanisms are needed in the model to account for the simultaneous adjustment of morphogen distribution shape and amplitude.

Examples of active modulation: the BMP signaling gradient in *Xenopus laevis*

In a famous experiment, Spemann and Mangold demonstrated that the salamander embryo responds to transplantation of the dorsal blastopore lip to the ventral side of the embryo by forming a Siamese twin (Spemann and Mangold, 1924). Experiments on *Xenopus* later revealed adaptation of patterning to variations in overall size (Cooke, 1981). For example, if pre-gastrula embryos are reduced in size by removal of ventral cells, normal proportions of these elements are observed in embryos that are only 60% of normal size embryos at the late tailbud stage. Other experiments on *Xenopus* showed that the degree of regulation depends strongly on the stage of development: perturbations up to the eight-cell stage may or may not produce functional adults (Kageura and Yamana, 1983; Kageura and Yamana, 1984), whereas the appropriate bisection at the blastula stage produces identical twins (De Robertis, 2006). Recently, much of the molecular underpinning of dorsoventral (DV) patterning in *Xenopus* has been discovered (reviewed by Plouhinec et al., 2011), and it is now known that interactions between BMPs and their inhibitors are involved in creating the body plan along the DV axis (Reversade and De Robertis, 2005). Thus, the question arises of whether the spatial patterning of morphogens generated by this network has the observed capacity for size adaptation after removal of tissue, or whether other components must be involved.

BMP patterning in *Xenopus* uses four BMPs: BMP2/4/7, and the BMP3-related ADMP (antidorsalizing morphogenetic protein) (Reversade and De Robertis, 2005) (Fig. 6C). The BMPs are known to diffuse in the extracellular space (Smith, 2009), and the first step in BMP signal transduction is binding to type I receptors. Upon BMP binding to type I receptors, the type II BMP receptors are recruited into an active heterotetrameric receptor-signaling complex. This complex initiates phosphorylation of Smad1/5/8, transcription factors that bind to the common Smad (Smad-4), translocate to the nucleus and initiate transcription of BMP target genes (Eivers et al., 2008; Schmierer et al., 2008), many of which encode factors that affect the spatial distribution of morphogens and regulatory molecules (Umulis et al., 2009).

BMP4/7 signaling is high at the ventral center and BMP4/7 expression is maintained via a positive-feedback loop that simultaneously represses the expression of BMP2 and ADMP (Inomata et al., 2008). BMP4 and BMP7 are inhibited by Chordin, and their expression is lowest in the dorsal organizer region, where BMP2 and ADMP expression are highest. The result is oppositely directed gradients of BMPs, and the total BMP signaling is determined by the sum of the four BMP concentrations.

The activities of BMP2/4/7 and ADMP are regulated by numerous extracellular BMP-binding proteins, metalloproteases, and feedback mechanisms, which interact to pattern the DV axis of the embryo properly in the face of a wide variety of perturbations, including the removal of a large amount of embryonic tissue (Sasai et al., 1994) (Fig. 6C). The BMPs are regulated by four inhibitors expressed in the Spemann organizer: Chordin (Chd), Noggin (Nog), Follistatin and Cerberus (Piccolo et al., 1996; Plouhinec and De Robertis, 2009). Chd and Nog both sequester BMPs in the extracellular space. Dorsally expressed Chd is itself under tight

regulation by other secreted factors, including twisted gastrulation (Tsg), BMP1 and the Tolloid homolog Xolloid-related (Xlr) (Piccolo et al., 1997; Oelgeschläger et al., 2000; Lee et al., 2006; Inomata et al., 2008). Xlr is expressed only in the ventral organizer, and its expression is maintained by high BMP signaling. Xlr cleaves Chd into fragments and creates a dorsal-high to ventral-low distribution of functional Chordin. The proteolytic processing of Chd appears to be largely independent of ligand binding, but it depends on two additional secreted molecules: Sizzled and ONT1 (Onichtchouk et al., 1999). Sizzled is a frizzled-related protein that is a competitive inhibitor of Xlr. High levels of Sizzled reduce Xlr activity, whereas low levels do not inhibit Xlr. Intriguingly, both the Xlr inhibitor Sizzled and Xlr are under positive-feedback transcriptional control by BMP signaling (Lee et al., 2006). The combination of Xlr and Sizzled feedback auto-regulates total processing of Chd by Xlr ventrally, and ONT1, a member of the olfactomedian family, attenuates Chd activity dorsally by enhancing Xlr activity (Inomata et al., 2008).

Interactions between Xlr, Chd, ONT1, Sizzled and extracellular BMPs give rise to spatial variation of BMP signaling that is high ventrally and low dorsally. A mathematical model based primarily on the ADMP feedback network with Chordin shuttling was developed and analyzed to explain the mechanism of regulative re-scaling of dorsal half ligatures into well-proportioned adults (Ben-Zvi et al., 2008). In this model, ADMP rescues the loss of the ventral center and re-establishes the distribution of BMP activity along the ventral-dorsal axis of the developing embryo. Although containing only a small subset of the total network, the model appears to produce scaling results consistent with observations; however, the model does not recapitulate other properties of the gradient, such as morphogen range and amplitude (Francois et al., 2009).

An alternative conceptual model has also been proposed to explain scaling of BMP signaling in *Xenopus*, whereby Sizzled modulation of Chordin regulates the scaling of BMP signaling (Inomata et al., 2013). Here, the modulator that impacts the distribution of BMP signaling is Chordin, which is itself regulated by BMP signaling through the repression of Xlr by Sizzled, a positive-feedback target of BMP signaling (Fig. 8D). Thus, the two-level feedback regulation links the distribution of BMP signaling to the activity of the inhibitor of the signaling, whereby loss of *sizzled* by morpholino injection abolished scaling (Inomata et al., 2013). To investigate the modulator mechanism, a mathematical model based on the network shown in Fig. 6C demonstrated that feedback on Sizzled is essential for scaling; without it, scaling is not achieved and a broadening of the ventral domain results. The core mechanism consists of a double negative-feedback loop on Chordin lifetime, which results in an effective positive feedback on the modulator Chordin (Fig. 8D) with size information manifesting in the level of Sizzled (Fig. 8E). In contrast to an earlier model based on shuttling and ADMP feedback (Ben-Zvi et al., 2008), the Sizzled mechanism does not place constraints on preferential degradation by Chordin in complex with BMPs or a differential affinity between ADMP and BMP binding to Chordin. It is not clear from the new model whether aspects of ADMP feedback and Sizzled feedback work in concert to achieve additional performance objectives, such as robustness, and additional work is needed to compare and contrast the alternative schemes. An overarching theme, however, exists between the models for BMP scaling in *Xenopus* and active modulator mechanisms, such as the expander/repressor motif (Ben-Zvi et al., 2011). Feedback results in regulation of a modulator that contains information on the size of the system, and the modulator ultimately targets extracellular regulation of the morphogen range through Chordin.

Conclusions

The scaling of spatial patterns during development can result from any of a number of diverse mechanisms, and one can expect even more diversity to emerge from future discoveries. Despite the fact that the details of each scaling mechanism vary, they all must incorporate size information into the modulation of transport, reaction and production rates appropriately, in order to adjust the intrinsic scale and amplitude of the patterning species. The information on size may emerge from production of a modulator by all cells and its destruction at the boundary, or it may be produced in localized regions, either fixed *ab initio*, as in the passive mechanisms, or governed by interactions with other dynamically varying species, as in the active mechanisms. This adaptation of patterning to system size also reiterates the fact that trade-offs persist in biological mechanisms that achieve certain performance objectives (Lander, 2007). Proper scaling requires at least one species that properly encodes the size of the tissue being patterned in order that the distribution of other species be scale invariant. The trade-offs also provide important predictions that can be used to assay for molecules that might modulate morphogen scale. If they function primarily as a catalyst or an immobilizer, then the concentration of the modulator should decrease in proportion to the system size, whereas if the modulator functions primarily as an inhibitor or mobilizer, as in the ER motif, then the level of the modulator should increase relative to size. Although we focused on extracellular regulation of morphogens herein, scaling could also be achieved by intracellular processes or the integration of multiple inputs, such as from two morphogens being secreted from opposite ends of a growing tissue (McHale et al., 2006, Kang et al., 2012). The latter is but one example of many other mechanisms that should be considered when determining how a specific pathway accomplishes scale invariance.

It is currently an auspicious time to study the question of scale invariance in developing systems, because the increased use of quantitative imaging and mathematical modeling of morphogens and modulators may finally provide a mechanistic understanding of the ancient observation that: “Of animals, some resemble one another in all their parts...save only for a difference in the way of excess or defect...” (Aristotle, 1910).

Acknowledgements

We would like to thank the anonymous reviewers of the manuscript for insightful comments and recommendations.

Competing interests

The authors declare no competing financial interests.

Funding

This work was supported by the National Institutes of Health [GM29123 to H.G.O., and HD73156 to D.M.U.]. Deposited in PMC for release after 12 months.

Supplementary material

Supplementary material available online at
http://dev.biologists.org/lookup/suppl/doi:10.1242/dev.100511/-/DC1

References

Alon, U. (2007). *An Introduction to Systems Biology: Design Principles of Biological Circuits*, Vol. 10. Boca Raton, FL: CRC Press.

Aristotle (1910). *Historia Animalium* (Translation by D’Arcy Wentworth Thompson). Oxford: Clarendon Press.

Ben-Zvi, D. and Barkai, N. (2010). Scaling of morphogen gradients by an expansion-repression integral feedback control. *Proc. Natl. Acad. Sci. USA* **107**, 6924-6929.

Ben-Zvi, D., Shilo, B.-Z., Fainsod, A. and Barkai, N. (2008). Scaling of the BMP morphogen activation gradient in Xenopus embryos. *Nature* **453**, 1205-1211.

Ben-Zvi, D., Pyrowolakis, G., Barkai, N. and Shilo, B. Z. (2011). Expansion-repression mechanism for scaling the Dpp activation gradient in Drosophila wing imaginal discs. *Curr. Biol.* **21**, 1391-1396.

Bergmann, S., Sandler, O., Sberro, H., Shnider, S., Schejter, E., Shilo, B. Z. and Barkai, N. (2007). Pre-steady-state decoding of the Bicoid morphogen gradient. *PLoS Biol.* **5**, e46.
Bollenbach, T., Kruse, K., Pantazis, P., González-Gaitán, M. and Jülicher, F. (2005). Robust formation of morphogen gradients. *Phys. Rev. Lett.* **94**, 018103.
Bollenbach, T., Pantazis, P., Kicheva, A., Bökel, C., González-Gaitán, M. and Jülicher, F. (2008). Precision of the Dpp gradient. *Development* **135**, 1137-1146.
Chahda, J. S., Sousa-Neves, R., Mizutani, C. M. and Ma, J. (2013). Variation in the dorsal gradient distribution is a source for modified scaling of germ layers in Drosophila. *Curr. Biol.* **23**, 710-716.
Cheung, D., Miles, C., Kreitman, M. and Ma, J. (2011). Scaling of the Bicoid morphogen gradient by a volume-dependent production rate. *Development* **138**, 2741-2749.
Cooke, J. (1981). Scale of body pattern adjusts to available cell number in amphibian embryos. *Nature* **290**, 775-778.
Coppey, M., Berezhkovskii, A. M., Kim, Y., Boettiger, A. N. and Shvartsman, S. Y. (2007). Modeling the bicoid gradient: diffusion and reversible nuclear trapping of a stable protein. *Dev. Biol.* **312**, 623-630.
Coppey, M., Boettiger, A. N., Berezhkovskii, A. M. and Shvartsman, S. Y. (2008). Nuclear trapping shapes the terminal gradient in the Drosophila embryo. *Curr. Biol.* **18**, 915-919.
Cordingley, J. E., Sundaresan, S. R., Fischhoff, I. R., Shapiro, B., Ruskey, J. and Rubenstein, D. I. (2009). Is the endangered Grevy's zebra threatened by hybridization? *Anim. Conserv.* **12**, 505-513.
Crocker, J., Tamori, Y. and Erives, A. (2008). Evolution acts on enhancer organization to fine-tune gradient threshold readouts. *PLoS Biol.* **6**, e263.
De Robertis, E. M. (2006). Spemann's organizer and self-regulation in amphibian embryos. *Nat. Rev. Mol. Cell Biol.* **7**, 296-302.
Dou, W., Zhang, D., Jung, Y., Cheng, J. X. and Umulis, D. M. (2012). Label-free imaging of lipid-droplet intracellular motion in early Drosophila embryos using femtosecond-stimulated Raman loss microscopy. *Biophys. J.* **102**, 1666-1675.
Eivers, E., Fuentealba, L. C. and De Robertis, E. M. (2008). Integrating positional information at the level of Smad1/5/8. *Curr. Opin. Genet. Dev.* **18**, 304-310.
Foe, V. E. and Alberts, B. M. (1983). Studies of nuclear and cytoplasmic behaviour during the five mitotic cycles that precede gastrulation in Drosophila embryogenesis. *J. Cell Sci.* **61**, 31-70.
Francois, P., Vonica, A., Brivanlou, A. H. and Siggia, E. D. (2009). Scaling of BMP gradients in Xenopus embryos. *Nature* **461**, E1, discussion E2.
Gregor, T., Bialek, W., de Ruyter van Steveninck, R. R., Tank, D. W. and Wieschaus, E. F. (2005). Diffusion and scaling during early embryonic pattern formation. *Proc. Natl. Acad. Sci. USA* **102**, 18403-18407.
Gregor, T., Wieschaus, E. F., McGregor, A. P., Bialek, W. and Tank, D. W. (2007). Stability and nuclear dynamics of the bicoid morphogen gradient. *Cell* **130**, 141-152.
Gregor, T., McGregor, A. P. and Wieschaus, E. F. (2008). Shape and function of the Bicoid morphogen gradient in dipteran species with different sized embryos. *Dev. Biol.* **316**, 350-358.
Grimm, O. and Wieschaus, E. (2010). The Bicoid gradient is shaped independently of nuclei. *Development* **137**, 2857-2862.
Grimm, O., Coppey, M. and Wieschaus, E. (2010). Modelling the Bicoid gradient. *Development* **137**, 2253-2264.
Hamaratoglu, F., de Lachapelle, A. M., Pyrowolakis, G., Bergmann, S. and Affolter, M. (2011). Dpp signaling activity requires Pentagone to scale with tissue size in the growing Drosophila wing imaginal disc. *PLoS Biol.* **9**, e1001182.
Hecht, I., Rappel, W. J. and Levine, H. (2009). Determining the scale of the Bicoid morphogen gradient. *Proc. Natl. Acad. Sci. USA* **106**, 1710-1715.
Hengenius, J. B., Gribskov, M., Rundell, A. E., Fowlkes, C. C. and Umulis, D. M. (2011). Analysis of gap gene regulation in a 3D organism-scale model of the Drosophila melanogaster embryo. *PLoS ONE* **6**, e26797.
Hillen, T. and Othmer, H. G. (2002). The diffusion limit of transport equations 2: Chemotaxis Equations. *SIAM J. Appl. Math.* **62**, 1222-1250.
Houchmandzadeh, B., Wieschaus, E. and Leibler, S. (2002). Establishment of developmental precision and proportions in the early Drosophila embryo. *Nature* **415**, 798-802.
Inomata, H., Haraguchi, T. and Sasai, Y. (2008). Robust stability of the embryonic axial pattern requires a secreted scaffold for chordin degradation. *Cell* **134**, 854-865.
Inomata, H., Shibata, T., Haraguchi, T. and Sasai, Y. (2013). Scaling of dorsal-ventral patterning by embryo size-dependent degradation of Spemann's organizer signals. *Cell* **153**, 1296-1311.
Jaeger, J. (2011). The gap gene network. *Cell. Mol. Life Sci.* **68**, 243-274.
Jaeger, J., Surkova, S., Blagov, M., Janssens, H., Kosman, D., Kozlov, K. N., Manu, Myasnikova, E., Vanario-Alonso, C. E., Samsonova, M. et al. (2004). Dynamic control of positional information in the early Drosophila embryo. *Nature* **430**, 368-371.
Kageura, H. and Yamana, K. (1983). Pattern regulation in isolated halves and blastomeres of early Xenopus laevis. *J. Embryol. Exp. Morphol.* **74**, 221-234.
Kageura, H. and Yamana, K. (1984). Pattern regulation in defect embryos of Xenopus laevis. *Dev. Biol.* **101**, 410-415.
Kang, H., Zheng, L. and Othmer, H. G. 2012. The efect of the signaling scheme on the robustness of pattern formation in development. *J. R. Soc. Interface Focus*. DOI: 10.1098/rsfs.2011.0116.
Kondo, S. and Asai, R. (1995). A reaction-diffusion wave on the skin of the marine angelfish Pomacan-thus. *Nature* **376**, 765-768.
Kruse, K., Pantazis, P., Bollenbach, T., Jülicher, F. and González-Gaitán, M. (2004). Dpp gradient formation by dynamin-dependent endocytosis: receptor trafficking and the diffusion model. *Development* **131**, 4843-4856.
Lander, A. D. (2007). Morpheus unbound: reimagining the morphogen gradient. *Cell* **128**, 245-256.
Lee, H. X., Ambrosio, A. L., Reversade, B. and De Robertis, E. M. (2006). Embryonic dorsal-ventral signaling: secreted frizzled-related proteins as inhibitors of tolloid proteinases. *Cell* **124**, 147-159.
Li, Y. and Tower, J. (2009). Adult-specific over-expression of the Drosophila genes magu and hebe increases life span and modulates late-age female fecundity. *Mol. Genet. Genomics* **281**, 147-162.
Little, S. C., Tkačik, G., Kneeland, T. B., Wieschaus, E. F. and Gregor, T. (2011). The formation of the Bicoid morphogen gradient requires protein movement from anteriorly localized mRNA. *PLoS Biol.* **9**, e1000596.
Lott, S. E., Kreitman, M., Palsson, A., Alekseeva, E. and Ludwig, M. Z. (2007). Canalization of segmentation and its evolution in Drosophila. *Proc. Natl. Acad. Sci. USA* **104**, 10926-10931.
Manu, Surkova, S., Spirov, A. V., Gursky, V. V., Janssens, H., Kim, A. R., Radulescu, O., Vanario-Alonso, C. E., Sharp, D. H., Samsonova, M. and Reinitz, J. (2009). Canalization of gene expression and domain shifts in the Drosophila blastoderm by dynamical attractors. *PLoS. Comut. Biol.* **5**, e1000303.
McHale, P., Rappel, W. J. and Levine, H. (2006). Embryonic pattern scaling achieved by oppositely directed morphogen gradients. *Phys. Biol.* **3**, 107-120.
Miles, C. M., Lott, S. E., Hendriks, C. L., Ludwig, M. Z., Manu, Williams, C. L. and Kreitman, M. (2011). Artificial selection on egg size perturbs early pattern formation in Drosophila melanogaster. *Evolution* **65**, 33-42.
Milo, R., Shen-Orr, S., Itzkovitz, S., Kashtan, N., Chklovskii, D. and Alon, U. (2002). Network motifs: simple building blocks of complex networks. *Sci. STKE* **298**, 824-827.
Mizutani, C. M. and Sousa-Neves, R. (2010). Mechanisms and evolution of dorsal-ventral patterning. *Evol. Biol.* **2010**, 159-177.
Müller, P., Rogers, K. W., Yu, S. R., Brand, M. and Schier, A. F. (2013). Morphogen transport. *Development* **140**, 1621-1638.
Oelgeschläger, M., Larraín, J., Geissert, D. and De Robertis, E. M. (2000). The evolutionarily conserved BMP-binding protein Twisted gastrulation promotes BMP signalling. *Nature* **405**, 757-763.
Onichtchouk, D., Chen, Y. G., Dosch, R., Gawantka, V., Delius, H., Massagué, J. and Niehrs, C. (1999). Silencing of TGF-beta signalling by the pseudoreceptor BAMBI. *Nature* **401**, 480-485.
Othmer, H. G. (1983). A continuum model for coupled cells. *J. Math. Biol.* **17**, 351-369.
Othmer, H. G. and Pate, E. F. (1980). Scale-invariance in reaction-diffusion models of spatial pattern formation. *Proc. Natl. Acad. Sci. USA* **77**, 4180-4184.
Othmer, H. G. and Scriven, L. E. (1969). Interactions of reaction and diffusion in open systems. *Ind. Eng. Chem. Fundamen.* **8**, 302-315.
Othmer, H. G. and Scriven, L. E. (1971). Instability and dynamic pattern in cellular networks. *J. Theor. Biol.* **32**, 507-537.
Othmer, H. G., Painter, K., Umulis, D. and Xue, C. (2009). The intersection of theory and application in biological pattern formation. *Math. Model. Nat. Phenom.* **4**, 3-79.
Painter, K. J., Maini, P. K. and Othmer, H. G. (1999). Stripe formation in juvenile *Pomacanthus* explained by a generalized turing mechanism with chemotaxis. *Proc. Natl. Acad. Sci. USA* **96**, 5549-5554.
Piccolo, S., Sasai, Y., Lu, B. and De Robertis, E. M. (1996). Dorsoventral patterning in Xenopus: inhibition of ventral signals by direct binding of chordin to BMP-4. *Cell* **86**, 589-598.
Piccolo, S., Agius, E., Lu, B., Goodman, S., Dale, L. and De Robertis, E. M. (1997). Cleavage of Chordin by Xolloid metalloprotease suggests a role for proteolytic processing in the regulation of Spemann organizer activity. *Cell* **91**, 407-416.
Plouhinec, J. L. and De Robertis, E. M. (2009). Systems biology of the self-regulating morphogenetic gradient of the Xenopus gastrula. *Cold Spring Harb. Perspect. Biol.* **1**, a001701.
Plouhinec, J. L., Zakin, L. and De Robertis, E. M. (2011). Systems control of BMP morphogen flow in vertebrate embryos. *Curr. Opin. Genet. Dev.* **21**, 696-703.
Reversade, B. and De Robertis, E. M. (2005). Regulation of ADMP and BMP2/4/7 at opposite embryonic poles generates a self-regulating morphogenetic field. *Cell* **123**, 1147-1160.
Roy, S., Hsiung, F. and Kornberg, T. B. (2011). Specificity of Drosophila cytonemes for distinct signaling pathways. *Science* **332**, 354-358.
Sasai, Y., Lu, B., Steinbeisser, H., Geissert, D., Gont, L. K. and De Robertis, E. M. (1994). Xenopus chordin: a novel dorsalizing factor activated by organizer-specific homeobox genes. *Cell* **79**, 779-790.
Schmierer, B., Tournier, A. L., Bates, P. A. and Hill, C. S. (2008). Mathematical modeling identifies Smad nucleocytoplasmic shuttling as a dynamic signal-interpreting system. *Proc. Natl. Acad. Sci. USA* **105**, 6608-6613.
Shimmi, O., Umulis, D., Othmer, H. G. and O'Connor, M. B. (2005). Facilitated transport of a Dpp/Scw heterodimer by Sog/Tsg leads to robust patterning of the Drosophila blastoderm embryo. *Cell* **120**, 873-886.
Shingleton, A. W., Frankino, W. A., Flatt, T., Nijhout, H. F. and Emlen, D. J. (2007). Size and shape: the developmental regulation of static allometry in insects. *Bioessays* **29**, 536-548.
Smith, J. C. (2009). Forming and interpreting gradients in the early Xenopus embryo. *Cold Spring Harb. Perspect. Biol.* **1**, a002477.
Spemann, H. and Mangold, H. (1924). Uber induktion von embryonalanlagen durch implantation artfremder organisatoren. *Wilhelm Roux's Arch. Entwickl. Mech. Org.* **100**, 599-638.
Turing, A. M. (1952). The chemical basis of morphogenesis. *Philos. Trans. R. Soc. B* **237**, 37-72.

Umulis, D. M. (2009). Analysis of dynamic morphogen scale invariance. *J. R. Soc. Interface* **6**, 1179-1191.
Umulis, D. M. and Othmer, H. G. (2013). Scale invariance of morphogen-mediated patterning by flux optimization. In *Proceedings of the 5th International Conference on BioMedical Engineering and Informatics, 2012*. IEEE.
Umulis, D., O'Connor, M. B. and Othmer, H. G. (2008). Robustness of embryonic spatial patterning in *Drosophila melanogaster*. *Curr. Top. Dev. Biol.* **81**, 65-111.
Umulis, D., O'Connor, M. B. and Blair, S. S. (2009). The extracellular regulation of bone morphogenetic protein signaling. *Development* **136**, 3715-3728.
Umulis, D. M., Shimmi, O., O'Connor, M. B. and Othmer, H. G. (2010). Organism-scale modeling of early Drosophila patterning via bone morphogenetic proteins. *Dev. Cell* **18**, 260-274.
Vuilleumier, R., Springhorn, A., Patterson, L., Koidl, S., Hammerschmidt, M., Affolter, M. and Pyrowolakis, G. (2010). Control of Dpp morphogen signalling by a secreted feedback regulator. *Nat. Cell Biol.* **12**, 611-617.
Wang, Y. C. and Ferguson, E. L. (2005). Spatial bistability of Dpp-receptor interactions during Drosophila dorsal-ventral patterning. *Nature* **434**, 229-234.
Wartlick, O. and González-Gaitán, M. (2011). The missing link: implementation of morphogenetic growth control on the cellular and molecular level. *Curr. Opin. Genet. Dev.* **21**, 690-695.
Wartlick, O., Mumcu, P., Kicheva, A., Bittig, T., Seum, C., Jülicher, F. and González-Gaitán, M. (2011). Dynamics of Dpp signaling and proliferation control. *Science* **331**, 1154-1159.
Wolpert, L. (1969). Positional information and the spatial pattern of cellular differentiation. *J. Theor. Biol.* **25**, 1-47.

Box S1. Equations for morphogen patterning by reaction and transport

While many models are based on one dimension, patterning often occurs in two or three dimensions. Therefore, we present the equations in a general form starting from the basic physical processes of molecular flux by diffusion and advection, a process whereby molecules are swept along by the cytoplasm of a cell or extracellular flow as occurs to some degree in the syncytial blastoderm embryo for Drosophila melanogaster. For morphogen patterning mediated by reaction and transport, the continuity equation, combined with a constitutive equation for molecular flux take following form in Cartesian coordinates:

(S1.1) $$\frac{\partial c_i}{\partial t} + \nabla \bullet \mathbf{j}_i = R_i(\mathbf{x}, \mathbf{c}, \mathbf{p})$$ Continuity equation

(S1.2) $$\mathbf{j}_i = -D_i(\mathbf{x}, \mathbf{c}, \mathbf{p})\nabla c_i + \mathbf{v}c_i + B.C.s$$ Flux equation (Constitutive equation w/ convection)

(S1.3) $$\nabla = \hat{\mathbf{e}}_x \frac{\partial}{\partial x} + \hat{\mathbf{e}}_y \frac{\partial}{\partial y} + \hat{\mathbf{e}}_z \frac{\partial}{\partial z}$$ Definition of gradient

Here c_i is the concentration of species i, $\mathbf{j}$ is the molecular flux defined by a constitutive equation for diffusion based on Fick's law and advection, R_i is the reaction rate for species i, $\mathbf{x}$ is the vector for the spatial coordinate, $\mathbf{v}$ is the velocity of cytoplasm or growing tissue that contributes to advection, $\mathbf{c}$ is the vector of concentrations of all molecular species $i=1\ldots n$ that interact in the network (receptors, inhibitors, co-factors, etc.), and $\mathbf{p}$ is the vector of parameters and physical rate constants. Bold-face font indicates a vector quantity. B.C.'s denotes boundary conditions.

If we limit our analysis to one spatial dimension, assume D does not depend explicitly on position, but does depend on the concentration of molecular species (e.g. modulator molecules), the above equations can be simplified to the general reaction-transport equations for morphogen patterning by component i in 1D:

(S1.4) $$\frac{\partial c_i}{\partial t} + v_x \frac{\partial c_i}{\partial x} = \frac{\partial}{\partial x}\left(D_i(\mathbf{c}(x), \mathbf{p}) \frac{\partial c_i}{\partial x} \right) + R_i(\mathbf{x}, \mathbf{c}, \mathbf{p})$$

(S1.5) $$\frac{\partial c_i}{\partial t} + v_x \frac{\partial c_i}{\partial x} = D_i(\mathbf{c}(x), \mathbf{p}) \frac{\partial^2 c_i}{\partial x^2} + \left[\sum_j \frac{\partial D_i}{\partial c_j} \frac{\partial c_j}{\partial x} \right] \frac{\partial c_i}{\partial x} + R_i(\mathbf{x}, \mathbf{c}, \mathbf{p})$$

If molecular diffusion is independent of modulation and there is no advection, then the equation can be simplified further into the most common form of reaction-transport equation analyzed in morphogen patterning:

(S1.6) $$\frac{\partial c_i}{\partial t} = D_i \frac{\partial^2 c_i}{\partial x^2} + R_i(\mathbf{x}, \mathbf{c}, \mathbf{p})$$

In Box S3 example solutions to the steady-state form of this equation with different boundary conditions are shown and in Box S4 we consider the case when diffusion depends on modulators that may vary in space.

Box S2. Scale-invariance of reaction-diffusion equations for morphogen patterning

The scaling properties of a system of partial differential equations can be easily investigated by dimensional analysis. Consider equations S2.1-S2.3 for a secreted morphogen with boundary conditions, and assume an initial spatial distribution of zero morphogen, which gives:

(S2.1) $$\frac{\partial m}{\partial t} = \frac{\partial}{\partial x}\left(D_m \frac{\partial m(x,t)}{\partial x}\right) + k_m R(m)$$

(S2.2) $$-D_m \frac{\partial m(x,t)}{\partial x} = q, \qquad x = 0$$

(S2.3) $$\frac{\partial m(x,t)}{\partial x} = 0, \qquad x = L$$

To understand scaling of the solution, we choose a time scale T, we define the dimensionless time variable τ and a dimensionless space variable ξ as $\tau = t/T$ and $\xi = x/L$ and we rewrite the equations in terms of these variables. The resulting equations are:

(S2.4) $$\left(\frac{1}{k_m T}\right)\frac{\partial m}{\partial \tau} = \left(\frac{D_m}{k_m L^2}\right)\frac{\partial^2 m}{\partial \xi^2} + R(m).$$

(S2.5) $$-\frac{\partial m(\xi,\tau)}{\partial \xi} = \frac{qL}{D_m}, \qquad \xi = 0$$

(S2.6) $$\frac{\partial m(\xi,\tau)}{\partial \xi} = 0, \qquad \xi = 1$$

These equations contain dimensionless groups that affect the solution, and the length of the system appears in some of these groups. The solution $m(\xi, \tau)$ of the rescaled equations will be scale-invariant only if there is no explicit dependence on L in these equations. There are two cases that arise, depending on whether or not the input flux j vanishes.

1. If $q=0$, then there are two dimensionless groups: $k_m T$ and $D_m/k_m L^2$. The first is a dimensionless reaction time scale, and the second a dimensionless diffusion coefficient. Both the transient evolution and the steady-state morphogen pattern will be independent of the system size if these groups are independent of L, which can be achieved as follows:
   - Fix k_m, select $T=k_m^{-1}$ and modulate $D_m \propto L^2$
   - Choose $T=k_m^{-1}$, modulate $k_m \propto L^{-2}$ and fix D_m
   - Any combination of modulating D_m and k_m to make the dimensionless groups independent of L.

2. If $q \neq 0$ then there are three dimensionless groups: $k_m T$, $D_m/k_m L^2$, and $Q = qL/D_m$ and each of these must be modulated so that they are L-independent. This can be achieved by:
   - Fix k_m, select $T=k_m^{-1}$ and modulate $D_m \propto L^2$, $q \propto L$
   - Fix D_m, choose $T=k_m^{-1}$, modulate $k_m \propto L^{-2}$ and input flux $q \propto L^{-1}$
   - More generally, any combination of modulation that makes the dimensionless groups independent of L will lead to scale-invariance. A balanced modulation of transport and reaction, in which $D_m \propto L$ and $k_m \propto L^{-1}$ may be optimal, in that no scaling of the input flux is required.

Box S3. Mechanisms of scale-invariance for morphogen-mediated patterning

Starting with the 1D equivalent of continuity equation S1.1 and constitutive equation in S1.2 with simple linear decay and constant diffusion, the requirements for scale-invariance of morphogen patterning are readily apparent.

(S3.1) $$\frac{\partial m}{\partial t}+v_x\frac{\partial m}{\partial x}=D_m\frac{\partial^2 m}{\partial x^2}-k_m m \quad where \quad m=m\left(x,t\right)$$

(S3.2) $$q_{in}=-D_m\frac{\partial m}{\partial x}\left(0,t\right)+v_x m\left(0,t\right) \qquad or \qquad m\left(0,t\right)=m_0$$

(S3.3) $$q_{out}=-D_m\frac{\partial m}{\partial x}\left(L,t\right)+v_x m\left(L,t\right) \qquad or \qquad m\left(L,t\right)=m_1$$

(S3.4) $$m\left(x,0\right)=f\left(x\right)$$

Here q_{in} is the input molecular flux, v_x is the velocity in the x direction, and k_m is the decay rate of the morphogen. If we restrict ourselves to identifying conditions at steady-state or quasi-steady state, (S3.1) through (S3.3) provide easily identifiable conditions for scale invariance that vary depending on the contributions from boundary conditions and the type of molecular transport. First, (S3.1)-(S3.3) are scaled by the length. Defining $\xi = x/L$ gives the following:

(S3.5) $$0=\frac{D_m}{L^2}\frac{d^2m}{d\xi^2}-\frac{v_x}{L}\frac{dm}{d\xi}-k_m m$$

(S3.6) $$q_{in}=-\frac{D_m}{L}\frac{dm}{d\xi}\left(0\right)+v_x m\left(0\right) \qquad or \qquad m\left(0\right)=m_0$$

(S3.7) $$q_{out}=-\frac{D_m}{L}\frac{dm}{d\xi}\left(1\right)+v_x m\left(1\right) \qquad or \qquad m\left(1\right)=m_1$$

A Scaling of models with advective transport

Advection-dominated transport leads to the following equation:

$$\frac{dm}{d\xi}=-\frac{k_m L}{v_x}m$$
$$q_{in}=v_x m\left(0\right)$$

Note we drop boundary condition S3.7.
This has the solution:

$$m\left(\xi\right)=\frac{q_{in}}{v_x}\exp\left(-\frac{k_m L}{v_x}\xi\right)$$

which is scale invariant for:

$$k_m \propto L^{-1}$$
$$or \;\; v_x \propto L;\;\; j_{in} \propto L$$

B Boundary condition mediated scaling

In the absence of advection and decay, with fixed concentration endpoints, (S3.5)-(S3.7) simplify to:

$$\frac{d^2m}{d\xi^2}=0$$
$$m\left(0\right)=m_0$$
$$m\left(1\right)=m_1$$

This has the solution:

$$m\left(\xi\right)=\left(m_1-m_0\right)\xi+m_0$$

which is scale invariant automatically. Note that constant concentration endpoints are unlikely and haven't been observed.

C Scaling of diffusion-decay models of patterning

Reaction and diffusion with flux at the source and no flux elsewhere (S3.5)-(S3.7) simplify to:

$$\frac{d^2m}{d\xi^2}=\lambda^2 m;\quad \lambda^2=\frac{k_m L^2}{D_m}$$
$$-\frac{dm}{d\xi}\left(0\right)=Q;\;\; \frac{dm}{d\xi}\left(1\right)=0$$

This has the solution:

$$m\left(\xi\right)=\frac{Q}{\lambda}\left[\frac{e^{\lambda\left(2-\xi\right)}+e^{\lambda\xi}}{e^{2\lambda}-1}\right]$$

Or, for large λ (large k_m, small D_m):

$$m\left(\xi\right)\approx\frac{q}{\sqrt{k_m D_m}}\exp\left(-\sqrt{\frac{k_m L^2}{D_m}}\xi\right)$$

which is scale invariant for:

$$\left(k_m/D_m\right)\propto L^{-2} \;\; and \;\; q\propto\sqrt{k_m D_m}$$

Box S4. Modulation of morphogen scale.

One can envision many mechanisms of modulator activity that lead to morphogen scale invariance. Consider the special case of equation 8-9 in the text in which the modulator activity affects both reaction and diffusion as indicated below:

(S4.1) $$D_{m0}f\left(M\right)=D_m\left(M\right)\equiv D_m^M \quad and \quad \kappa R_m\left(m,M\right)=\kappa_M\left(M\right)r_m\left(m\right)\equiv\kappa_M r_m\left(m\right)$$

where D_{m0} is the intrinsic morphogen diffusion rate. Then equation 8 can be re-written as:

(S4.2) $$\frac{\partial m}{\partial t}=\frac{1}{L^2}\frac{\partial}{\partial\xi}\left(D_m^M\frac{\partial m}{\partial\xi}\right)+\kappa_M r_m\left(m\right)$$

If M is established by a boundary-sink mechanism, then D_m^M is space dependent and the level of M grows in proportion to L^2, ensuring scale-invariance (see Example 2, below). If M is spatially uniform and constant, then (S4.2) can be reduced to:

(S4.3) $$\frac{1}{\kappa_M}\frac{\partial m}{\partial t}=\left(\frac{D_m^M}{\kappa_M L^2}\right)\frac{\partial^2 m}{\partial\xi^2}+r_m\left(m\right)$$

The system will be scale-invariant if $D_m^M\kappa_M^{-1}$ is proportional to L^2. There are many mechanisms that ensure $D_m^M\kappa_M^{-1}\propto L^2$ and the specific molecular actions differ greatly between biological contexts. The following examples illustrate how M must vary for proper D_m^M and κ_M scaling.

Example 1: Enhancer/Immobilizer

If the modulator's molecular function is to hinder diffusion and/or enhance reaction rates, then scaling can be ensured if M decreases in proportion to the tissue size by an appropriate amount. Suppose that the effect of M on the rates are as shown:

(S4.4) $$\frac{\partial m}{\partial t}=\frac{1}{L^2}\frac{\partial}{\partial\xi}\left(\underbrace{\frac{D_{m0}}{1+\alpha_1 M}}_{D_m^M}\frac{\partial m}{\partial\xi}\right)-\underbrace{\kappa\cdot\left(1+\alpha_2 M\right)}_{\kappa_M}\cdot r_m\left(m\right)$$

where the modulator can slow diffusion, enhance reactions, or a combination of both. General requirements to ensure scaling by modulation of D_m^M and κ_M, and parameters that provide the requirement in (S4.4) are below:

Table S4.1	*Example*		*General*		
Description	α_1	α_2	D_m^M	κ_M	M
RXN Enhancer	0	>0	const	$\propto M$	$\propto L^{-2}$
Immobilizer	>0	0	$\propto M^{-1}$	const	$\propto L^{-2}$
Combination	>0	>0	$\propto M^{-1}$	$\propto M$	$\propto L^{-1}$

Suppose a population of cells secretes a modulator M from a source $q(\mathbf{x})$, the modulator diffuses, decays linearly and no flux occurs across the boundaries. This gives:

(S4.5) $$\frac{\partial M}{\partial t}=D_M\nabla^2 M-k\cdot M+j\left(\mathbf{x}\right)$$

Then the average concentration of modulator at steady-state is given by:

(S4.6) $$M_{avg}=\frac{1}{k\theta}\int_\Omega j\left(\mathbf{x}\right)d\Omega \quad where\ \theta=\begin{cases}\propto L & 1D\\ \propto L^2 & 2D\\ \propto L^3 & 3D\end{cases}$$

Thus a line source in 2D yields $M_{avg}\propto L^{-1}$, whereas a finite number of secreting cells in 2D yields $M_{avg}\propto L^{-2}$. If diffusion is very rapid, then $M(x)\approx M_{avg}$ and scaling can be ensured by the "Combination" mechanism (see Table S4.1) for a line source of M, or by the RXN Enhancer or Immobilizer mechanism for a finite size source of M and isometric tissue expansion.

Example 2: Inhibitor/Mobilizer

If the modulator's molecular function is to enhance diffusion and/or hinder reaction rates, then scaling can be ensured if M increases in proportion to the tissue size by an appropriate amount. Consider the action of M on the morphogen by the following equation:

(S4.7) $$\frac{\partial m}{\partial t}=\frac{1}{L^2}\frac{\partial}{\partial\xi}\left(\underbrace{D_{m0}\cdot\left(1+\alpha_1 M\right)}_{D_m^M}\frac{\partial m}{\partial\xi}\right)-\underbrace{\frac{\kappa}{1+\alpha_2 M}}_{\kappa_M}r_m\left(m\right)$$

where the modulator can speed up diffusion, hinder reactions, or a combination of both. General requirements to ensure scaling by modulation of D_m^M and κ_M, and parameters that provide the requirement in (S4.7) are below:

Table S4.2	*Example*		*General*		
Description	α_1	α_2	D_m^M	κ_M	M
RXN Inhibitor	0	>0	const	$\propto M^{-1}$	$\propto L^2$
Mobilizer	>0	0	$\propto M$	const	$\propto L^2$
Combination	>0	>0	$\propto M$	$\propto M^{-1}$	$\propto L^1$

Suppose that all cells in a system are identical and produce M at a constant rate j. If the concentration is zero at the ends due to rapid leaking of M out of the domain or active degradation, then this gives:

(S4.8) $$\frac{\partial M}{\partial t}=\frac{D_M}{L^2}\frac{\partial^2 M}{\partial\xi^2}+j \quad where\begin{cases}M\left(0,t\right)=0\\ M\left(L,t\right)=0\end{cases}$$

which has the steady-state solution:

(S4.9) $$M\left(\xi\right)=\frac{qL^2}{2D_M}\left(\xi-\xi^2\right)$$

Thus $M(\xi)\propto L^2 f(\xi)$, and although the distribution of modulator is non-uniform in space, the local level adjusts in proportion to L^2, which would ensure scaling by either the RXN inhibitor or the Mobilizer mechanisms in Table S4.2 (Pate and Othmer, 1984).

Box S5. How amplitude modulation can lead to adequate scaling

There are numerous examples of tissue patterning between organisms within a species and between species where the patterns provide some degree of scale invariance but key differences arise upon closer inspection. Within populations of Drosophila that were artificially selected into groups based on their egg size, scaling is predominately mediated by the total flux of molecules into the system. While the specific mechanisms for Bcd-mediated transport are still being worked out, the profile has been frequently described by a reaction diffusion model that produces an exponentially decaying spatial distribution at "quasi" steady-state. This takes the form of equation (S5.1):

$$m_i(\xi) \approx \frac{q}{\sqrt{k_m D_m}} \exp\left(-\sqrt{\frac{k_m}{D_m}} L\xi\right) \quad \text{(S5.1)}$$

Intriguingly, the measured decay constant is roughly constant between the population of large embryos (~645 microns long) and small embryos (~518 microns long). Instead the principle difference between profiles is the amount of measured Bcd protein intensity throughout the Anterior of the embryo. Thus, even though the extent or range of the profiles are very different, the Bcd distribution is scaled enough by an increase in the total amount of Bcd in the system. This represents "flux" or "concentration" optimization. If the flux (concentration) is regulated to reduce error in positional information, approximate scaling can be achieved for a number of systems. If the interpretation of the pattern takes place at only one spatial position by a threshold, then (S5.1) can be regulated for exact scaling at that lone position. If multiple thresholds are interpreted, then this mechanism would lead to error in the placement of those boundaries. Intriguingly, Bcd patterning within Drosophila seems to scale by flux optimization. Suppose that there is a critical threshold in the gradient (e.g. the boundary of Hbk gene expression) that occurs at ξ_T. Then the flux increase required for scaling at ξ_T can be calculated by equation (S5.2):

$$q_L(L) = q_0 \exp\left(\sqrt{\frac{k_m}{D_m}}(L - L_0)\xi_T\right) \quad \text{(S5.2)}$$

Taking the data from Cheung et al. with $(D/k)^{1/2}$ = 99 microns, assuming ξ_T =0.4 as the critical threshold in the embryo (near the Hbk boundary), and using L=645 for the large embryo and L_0=518 for the small embryo, the calculated optimal flux q_L is 67% greater than the flux in the small embryo q_0. This is remarkably close to the increase in amplitude measured for Bcd scaling of 66.9%. Thus, while the amplitude correlates with embryo volume, it also correlates with a flux or concentration optimization process. The error at other spatial positions away from the critical threshold can be calculated by:

$$\Delta\xi \equiv \xi_L - \xi = \left(1 - \frac{L_0}{L}\right)(\xi_T - \xi) \quad \text{(S5.3)}$$

Depending on the allowable variations in the spatial positions of gene expression $\Delta\xi$, equation S5.3 can be used to estimate the range of lengths where flux optimization provides sufficient scaling.